

FINITE ELEMENT COMPLEXES IN TWO DIMENSIONS

LONG CHEN AND XUEHAI HUANG

ABSTRACT. Two-dimensional finite element complexes with various smoothness, including the de Rham complex, the curldiv complex, the elasticity complex, and the divdiv complex, are systematically constructed in this work. First smooth scalar finite elements in two dimensions are developed based on a non-overlapping decomposition of the simplicial lattice and the Bernstein basis of the polynomial space. Smoothness at vertices is more than doubled than that at edges. Then the finite element de Rham complexes with various smoothness are devised using smooth finite elements with smoothness parameters satisfying certain relations. Finally, finite element elasticity complexes and finite element divdiv complexes are derived from finite element de Rham complexes by using the Bernstein-Gelfand-Gelfand (BGG) framework. Additionally, some finite element divdiv complexes are constructed without BGG framework. Dimension count plays an important role for verifying the exactness of two-dimensional finite element complexes.

1. INTRODUCTION

Hilbert complexes play a fundamental role in the theoretical analysis and the design of stable numerical methods for partial differential equations [5, 2, 3, 13]. Recently in [7] Arnold and Hu have developed a systematical approach to derive new complexes from well-understood differential complexes such as the de Rham complex. Complexes derived in [7] are involving Sobolev spaces. In this work we shall construct two-dimensional finite element complexes with various smoothness in a systematic way, including finite element de Rham complexes, finite element elasticity complexes, and finite element divdiv complexes etc.

We first construct smooth finite elements in two dimensions by a geometric approach, in which the simplicial lattice $\mathbb{T}_k^2 = \{\alpha = (\alpha_0, \alpha_1, \alpha_2) \in \mathbb{N}^{0:2} \mid \alpha_0 + \alpha_1 + \alpha_2 = k\}$ as the multi-index set with fixed length k is employed. The smoothness at vertices and edges are specified by parameters r^v and r^e , respectively. When $r^v \geq 2r^e$ and $k \geq 2r^v + 1$, we construct C^{r^e} -continuous finite element spaces using a non-overlapping decomposition (partition) of the simplicial lattice \mathbb{T}_k^2 and the Bernstein basis $\{\lambda^\alpha, \alpha \in \mathbb{T}_k^2\}$ of polynomial space \mathbb{P}_k , where λ is the barycentric coordinate.

We then move to the finite element de Rham complexes. Given three integer vectors $\mathbf{r}_0 = (r_0^v, r_0^e)$, $\mathbf{r}_1 = (r_1^v, r_1^e)$, $\mathbf{r}_2 = (r_2^v, r_2^e)$, assume $\mathbf{r}_0 = \mathbf{r}_1 + 1$, $\mathbf{r}_1 \geq -1$, $\mathbf{r}_2 \geq \max\{\mathbf{r}_1 - 1, -1\}$ satisfying $r_1^v \geq 2r_1^e + 1$, $r_2^v \geq 2r_2^e$. For $k \geq \max\{2r_1^v + 2, 2r_2^v + 2, 1\}$, we devise finite element de Rham complexes of various smoothness

$$(1) \quad \mathbb{R} \xrightarrow{\subset} \mathbb{V}_{k+1}^{\text{curl}}(\mathcal{T}_h; \mathbf{r}_0) \xrightarrow{\text{curl}} \mathbb{V}_k^{\text{div}}(\mathcal{T}_h; \mathbf{r}_1, \mathbf{r}_2) \xrightarrow{\text{div}} \mathbb{V}_{k-1}^{L^2}(\mathcal{T}_h; \mathbf{r}_2) \rightarrow 0,$$

The first author was supported by NSF DMS-1913080 and DMS-2012465.

The second author is the corresponding author. The second author was supported by the National Natural Science Foundation of China Project 12171300, the Natural Science Foundation of Shanghai 21ZR1480500, and the Fundamental Research Funds for the Central Universities 2019110066.

which is the finite element discretization of the de Rham complex

$$\mathbb{R} \xrightarrow{\subset} H^{r_0^e+1}(\Omega) \xrightarrow{\text{curl}} \mathbf{H}^{r_1^e+1, r_2^e+1}(\text{div}, \Omega) \xrightarrow{\text{div}} H^{r_2^e+1}(\Omega) \rightarrow 0,$$

where $H^s(\Omega)$ is the standard Sobolev space and

$$\mathbf{H}^{r_1^e+1, r_2^e+1}(\text{div}, \Omega) := \{\mathbf{v} \in \mathbf{H}(\text{div}, \Omega) : \mathbf{v} \in \mathbf{H}^{r_1^e+1}(\Omega, \mathbb{R}^2), \text{div } \mathbf{v} \in H^{r_2^e+1}(\Omega)\}.$$

Note that in two dimensions, by rotation of the vector field and differential operators, we also obtain the finite element de Rham complex

$$(2) \quad \mathbb{R} \xrightarrow{\subset} \mathbb{V}_{k+1}^{\text{grad}}(\mathcal{T}_h; \mathbf{r}_0) \xrightarrow{\text{grad}} \mathbb{V}_k^{\text{rot}}(\mathcal{T}_h; \mathbf{r}_1, \mathbf{r}_2) \xrightarrow{\text{rot}} \mathbb{V}_{k-1}^{L^2}(\mathcal{T}_h; \mathbf{r}_2) \rightarrow 0,$$

in which the space $\mathbb{V}_k^{\text{rot}}(\mathcal{T}_h; \mathbf{r}_1, \mathbf{r}_2)$ can find applications in Maxwell equation or fourth-order curl problems.

Several existing finite element de Rham complexes in two dimensions are special examples of (1) or (2), and summarized in the following table.

TABLE 1. Examples of finite element de Rham complexes.

\mathbf{r}_0	\mathbf{r}_1	\mathbf{r}_2	Results
(0, 0)	(-1, -1)	(-1, -1)	standard
(2, 1)	(1, 0)	(0, -1)	[23, Section 3]
(2, 1)	(1, 0)	(0, 0)	[23, Section 4]
(1, 0)	(0, -1)	(-1, -1)	[19, Section 2.2]
(0, 0)	(-1, -1)	(0, 0)	[27, Section 5.2.1]

Based on finite element de Rham complexes, we then use the Bernstein-Gelfand-Gelfand (BGG) framework [7] to construct more finite element complexes. For $\mathbf{r}_1 \geq -1$ and $\mathbf{r}_2 \geq \max\{\mathbf{r}_1 - 1, -1\}$ satisfying $r_1^v \geq 2r_1^e + 2$, $r_2^v \geq 2r_2^e$, and polynomial degree $k \geq \max\{2r_1^v + 3, 2r_2^v + 2\}$, we design the BGG diagram

$$\begin{array}{ccccccc} \mathbb{R} & \xrightarrow{\subset} & \mathbb{V}_{k+2}^{\text{curl}}(\mathbf{r}_1 + 2) & \xrightarrow{\text{curl}} & \mathbb{V}_{k+1}^{\text{div}}(\mathbf{r}_1 + 1) & \xrightarrow{\text{div}} & \mathbb{V}_k^{L^2}(\mathbf{r}_1) \longrightarrow 0 \\ & & & \nearrow \text{id} & & \nearrow -2 \text{sskw} & \\ \mathbb{R}^2 & \xrightarrow{\subset} & \mathbb{V}_{k+1}^{\text{curl}}(\mathbf{r}_1 + 1; \mathbb{R}^2) & \xrightarrow{\text{curl}} & \mathbb{V}_k^{\text{div}}(\mathbf{r}_1, \mathbf{r}_2; \mathbb{M}) & \xrightarrow{\text{div}} & \mathbb{V}_{k-1}^{L^2}(\mathbf{r}_2; \mathbb{R}^2) \longrightarrow 0 \end{array}$$

which leads to the finite element elasticity complex

$$\mathbb{P}_1 \xrightarrow{\subset} \mathbb{V}_{k+2}^{\text{curl}}(\mathbf{r}_1 + 2) \xrightarrow{\text{Air}} \mathbb{V}_k^{\text{div}}(\mathbf{r}_1, \mathbf{r}_2; \mathbb{S}) \xrightarrow{\text{div}} \mathbb{V}_{k-1}^{L^2}(\mathbf{r}_2; \mathbb{R}^2) \rightarrow 0.$$

Examples include the finite element elasticity complex in [19]: $\mathbf{r}_1 = (0, -1)$ and $\mathbf{r}_2 = (-1, -1)$, and the finite element Hessian complex in [15]: $\mathbf{r}_1 = (0, -1)$ and $\mathbf{r}_2 = (0, 0)$.

For $\mathbf{r}_1 \geq 0$, $\mathbf{r}_2 \geq \max\{\mathbf{r}_1 - 2, -1\}$, and $k \geq \max\{2r_1^v + 3, 2r_2^v + 3\}$, we build the BGG diagram

$$\begin{array}{ccccccc} \mathbb{R}^2 & \xrightarrow{\subset} & \mathbb{V}_{k+1}^{\text{curl}}(\mathbf{r}_1 + 1; \mathbb{R}^2) & \xrightarrow{\text{curl}} & \mathbb{V}_k^{\text{div div}^+}(\mathbf{r}_1, \mathbf{r}_2; \mathbb{M}) & \xrightarrow{\text{div}} & \mathbb{V}_{k-1}^{\text{div}}(\mathbf{r}_1 - 1, \mathbf{r}_2) \longrightarrow 0 \\ & & & \nearrow \text{mskw} & & \nearrow \text{id} & \\ \mathbb{R} & \xrightarrow{\subset} & \mathbb{V}_k^{\text{curl}}(\mathbf{r}_1) & \xrightarrow{\text{curl}} & \mathbb{V}_{k-1}^{\text{div}}(\mathbf{r}_1 - 1, \mathbf{r}_2) & \xrightarrow{\text{div}} & \mathbb{V}_{k-2}^{L^2}(\mathbf{r}_2) \longrightarrow 0 \end{array}$$

which leads to the finite element divdiv complex

$$\mathbf{RT} \xrightarrow{\subset} \mathbb{V}_{k+1}^{\text{curl}}(\mathbf{r}_1 + 1; \mathbb{R}^2) \xrightarrow{\text{sym curl}} \mathbb{V}_k^{\text{div div}^+}(\mathbf{r}_1, \mathbf{r}_2; \mathbb{S}) \xrightarrow{\text{div div}} \mathbb{V}_{k-2}^{L^2}(\mathbf{r}_2) \rightarrow 0,$$

where $\mathbb{V}_k^{\text{div div}^+}(\mathbf{r}_1, \mathbf{r}_2; \mathbb{S}) \subset \mathbf{H}(\text{div div}, \Omega; \mathbb{S}) \cap \mathbf{H}(\text{div}, \Omega; \mathbb{S})$. We recover the finite element divdiv complex in [15] when choosing $\mathbf{r}_1 = (1, 0)$ and $\mathbf{r}_2 = (0, 0)$. By the way, discrete elasticity complexes and rot rot complexes based on the Clough-Tocher split are constructed in [20], whose shape functions are piece-wise polynomials.

Since the BGG construction will change only the algebraic structure not the smoothness of the Sobolev spaces, some finite element complexes may not be derived from the current BGG framework. For $r_1^e = -1$, we construct two more finite element divdiv complexes

$$\mathbf{RT} \xrightarrow{\subset} \mathbb{V}_{k+1}^{\text{div}}\left(\begin{pmatrix} r_1^v + 1 \\ 0 \end{pmatrix}, \begin{pmatrix} r_1^v \\ 0 \end{pmatrix}\right) \xrightarrow{\text{sym curl}} \mathbb{V}_k^{\text{div div}^+}\left(\begin{pmatrix} r_1^v \\ -1 \end{pmatrix}, \mathbf{r}_2; \mathbb{S}\right) \xrightarrow{\text{div div}} \mathbb{V}_{k-2}^{L^2}(\mathbf{r}_2) \rightarrow 0,$$

and

$$\mathbf{RT} \xrightarrow{\subset} \mathbb{V}_{k+1}^{\text{curl}}\left(\begin{pmatrix} r_1^v + 1 \\ 0 \end{pmatrix}; \mathbb{R}^2\right) \xrightarrow{\text{sym curl}} \mathbb{V}_k^{\text{div div}}\left(\begin{pmatrix} r_1^v \\ -1 \end{pmatrix}, \mathbf{r}_2; \mathbb{S}\right) \xrightarrow{\text{div div}} \mathbb{V}_{k-2}^{L^2}(\mathbf{r}_2) \rightarrow 0,$$

where $\mathbb{V}_k^{\text{div div}}\left(\begin{pmatrix} r_1^v \\ -1 \end{pmatrix}, \mathbf{r}_2; \mathbb{S}\right) \subset \mathbf{H}(\text{div div}, \Omega; \mathbb{S})$ only. When choosing $\mathbf{r}_1 = (0, -1)$ and $\mathbf{r}_2 = -1$, we recover the finite element divdiv complex in [26], and the one in [14].

The rest of this paper is organized as follows. The de Rham complex and BGG framework are reviewed in Section 2. In Section 3 the geometric decomposition of C^m -conforming finite elements in two dimensions is studied. Finite element de Rham complexes with various smoothness are constructed in Section 4. More finite element complexes with or without BGG approach are developed in Section 5.

2. PRELIMINARY ON HILBERT COMPLEXES

A Hilbert complex is a sequence of Hilbert spaces $\{\mathcal{V}_i\}$ connected by a sequence of closed densely defined linear operators $\{d_i\}$

$$0 \longrightarrow \mathcal{V}_1 \xrightarrow{d_1} \mathcal{V}_2 \xrightarrow{d_2} \dots \xrightarrow{d_{n-2}} \mathcal{V}_{n-1} \xrightarrow{d_{n-1}} \mathcal{V}_n \longrightarrow 0,$$

satisfying the property $\text{img}(d_i) \subseteq \ker(d_{i+1})$. The complex is called an exact sequence if $\text{img}(d_i) = \ker(d_{i+1})$ for $i = 1, \dots, n$. We usually skip the first 0 in the complex and use the embedding operator to indicate d_1 is injective. We refer to [3] for more background on Hilbert complexes.

In this paper, we shall consider Hilbert complexes associated to a two-dimensional domain Ω and d_i are some differential operators of scalar, vector, or tensor functions. For scalar function v , denote

$$\text{mskw } v := \begin{pmatrix} 0 & -v \\ v & 0 \end{pmatrix}, \quad \text{curl } v := \begin{pmatrix} \frac{\partial v}{\partial x_2} & -\frac{\partial v}{\partial x_1} \end{pmatrix}^\top = (\text{grad } v)^\perp,$$

where $(a, b)^\perp = (b, -a)$ is the 90° rotation clockwise, and

$$\text{Air } v := \text{curl curl } v = \begin{pmatrix} \frac{\partial^2 v}{\partial x_2^2} & -\frac{\partial^2 v}{\partial x_1 \partial x_2} \\ -\frac{\partial^2 v}{\partial x_1 \partial x_2} & \frac{\partial^2 v}{\partial x_1^2} \end{pmatrix}.$$

Then $\text{div}(\text{mskw } v) = -\text{curl } v$. For vector function $\mathbf{v} = (v_1, v_2)$, denote

$$\text{rot } \mathbf{v} := \frac{\partial v_2}{\partial x_1} - \frac{\partial v_1}{\partial x_2} = \text{div } \mathbf{v}^\perp.$$

For tensor function $\boldsymbol{\tau} = \begin{pmatrix} \tau_{11} & \tau_{12} \\ \tau_{21} & \tau_{22} \end{pmatrix}$, denote

$$\begin{aligned} \text{sym } \boldsymbol{\tau} &:= \frac{1}{2}(\boldsymbol{\tau} + \boldsymbol{\tau}^\top), \quad \text{skw } \boldsymbol{\tau} := \frac{1}{2}(\boldsymbol{\tau} - \boldsymbol{\tau}^\top), \\ \text{sskw } \boldsymbol{\tau} &:= \text{mskw}^{-1} \circ \text{skw } \boldsymbol{\tau} = \frac{1}{2}(\tau_{21} - \tau_{12}). \end{aligned}$$

Clearly we have

$$(3) \quad \text{div } \boldsymbol{v} = 2 \text{sskw}(\text{curl } \boldsymbol{v}), \quad \text{rot } \boldsymbol{v} = 2 \text{sskw}(\text{grad } \boldsymbol{v}).$$

2.1. The de Rham complex. For a domain $\Omega \subseteq \mathbb{R}^2$, the de Rham complex is

$$(4) \quad \mathbb{R} \xrightarrow{\subset} H^1(\Omega) \xrightarrow{\text{curl}} \boldsymbol{H}(\text{div}, \Omega) \xrightarrow{\text{div}} L^2(\Omega) \rightarrow 0.$$

When Ω is simply connected, the de Rham complex (4) is exact. Restricted to one triangle, a polynomial de Rham complex is, for $k \geq 1$,

$$(5) \quad \mathbb{R} \xrightarrow{\subset} \mathbb{P}_{k+1}(T) \xrightarrow{\text{curl}} \mathbb{P}_k(T; \mathbb{R}^2) \xrightarrow{\text{div}} \mathbb{P}_{k-1}(T) \rightarrow 0,$$

where $\mathbb{P}_k(T)$ denotes the set of real valued polynomials defined on T of degree less than or equal to k , and $\mathbb{P}_k(T; \mathbb{X}) := \mathbb{P}_k(T) \otimes \mathbb{X}$ for \mathbb{X} being vector space \mathbb{R}^2 , tensor space \mathbb{M} , or symmetric tensor space \mathbb{S} . Given a triangulation \mathcal{T}_h of Ω , we shall construct finite element de Rham complex

$$(6) \quad \mathbb{R} \xrightarrow{\subset} \mathbb{V}_{k+1}^{\text{curl}}(\mathcal{T}_h) \xrightarrow{\text{curl}} \mathbb{V}_k^{\text{div}}(\mathcal{T}_h) \xrightarrow{\text{div}} \mathbb{V}_{k-1}^{L^2}(\mathcal{T}_h) \rightarrow 0.$$

Usually the spaces are constructed so that (6) is a complex, i.e., $\text{curl}(\mathbb{V}_{k+1}^{\text{curl}}(\mathcal{T}_h)) \subseteq \ker(\text{div}) \cap \mathbb{V}_k^{\text{div}}(\mathcal{T}_h)$ and $\text{div}(\mathbb{V}_k^{\text{div}}(\mathcal{T}_h)) \subseteq \mathbb{V}_{k-1}^{L^2}(\mathcal{T}_h)$ by construction. To verify the exactness, we rely on the following result.

Lemma 2.1. *Let*

$$(7) \quad \mathcal{V}_0 \xrightarrow{\subset} \mathcal{V}_1 \xrightarrow{d_1} \mathcal{V}_2 \xrightarrow{d_2} \mathcal{V}_3 \rightarrow 0,$$

be a complex, where \mathcal{V}_i are finite-dimensional linear spaces for $i = 0, \dots, 3$. Assume $\mathcal{V}_0 = \mathcal{V}_1 \cap \ker(d_1)$, and

$$(8) \quad \dim \mathcal{V}_0 - \dim \mathcal{V}_1 + \dim \mathcal{V}_2 - \dim \mathcal{V}_3 = 0.$$

If either $d_1 \mathcal{V}_1 = \mathcal{V}_2 \cap \ker(d_2)$ or $d_2 \mathcal{V}_2 = \mathcal{V}_3$, then complex (7) is exact.

Proof. Given the identity (8) and the relation $\mathcal{V}_0 = \mathcal{V}_1 \cap \ker(d_1)$, we prove the equivalence between $d_1 \mathcal{V}_1 = \mathcal{V}_2 \cap \ker(d_2)$ and $d_2 \mathcal{V}_2 = \mathcal{V}_3$ by dimension count. By $\mathcal{V}_0 = \mathcal{V}_1 \cap \ker(d_1)$,

$$\dim d_1 \mathcal{V}_1 = \dim \mathcal{V}_1 - \dim(\mathcal{V}_1 \cap \ker(d_1)) = \dim \mathcal{V}_1 - \dim \mathcal{V}_0.$$

Then it follows from (8) that

$$\begin{aligned} \dim(\mathcal{V}_2 \cap \ker(d_2)) - \dim d_1 \mathcal{V}_1 &= \dim \mathcal{V}_2 - \dim d_2 \mathcal{V}_2 - \dim \mathcal{V}_1 + \dim \mathcal{V}_0 \\ &= \dim \mathcal{V}_3 - \dim d_2 \mathcal{V}_2, \end{aligned}$$

as required. □

For example, consider the polynomial de Rham complex (5). The combinatory identity

$$(9) \quad 1 - \binom{k+3}{2} + 2\binom{k+2}{2} - \binom{k+1}{2} = 0$$

can be verified directly. The relation $\text{curl } \mathbb{P}_{k+1}(T) = \mathbb{P}_k(T; \mathbb{R}^2) \cap \ker(\text{div})$ is due to the fact: if $\text{grad } p \in \mathbb{P}_k(T; \mathbb{R}^2)$, then $p \in \mathbb{P}_{k+1}(T)$, and in two dimensions curl is a rotation of grad . Therefore complex (5) is exact.

2.2. BGG framework. In [22], the relation between the elasticity complex and the de Rham complex is established through BGG construction [9]. By mimicking such construction in the discrete case, Arnold, Falk and Winther [4] reconstruct the finite element elasticity complex in [8] from the finite element de Rham complex.

The BGG construction developed in [7] starts from two bounded Hilbert complexes $(\mathcal{V}_\bullet \otimes \mathbb{E}_\bullet, d_\bullet)$, $(\mathcal{V}_\bullet \otimes \tilde{\mathbb{E}}_\bullet, \tilde{d}_\bullet)$ and bounded linking maps $S_i = \text{id} \otimes s_i : \mathcal{V}_{i+1} \otimes \tilde{\mathbb{E}}_i \rightarrow \mathcal{V}_{i+1} \otimes \mathbb{E}_{i+1}$ for $i = 0, \dots, n-1$

$$(10) \quad \begin{array}{ccccccc} 0 & \longrightarrow & \mathcal{V}_0 \otimes \mathbb{E}_0 & \xrightarrow{d_0} & \mathcal{V}_1 \otimes \mathbb{E}_1 & \xrightarrow{d_1} & \cdots \xrightarrow{d_{n-1}} \mathcal{V}_n \otimes \mathbb{E}_n \longrightarrow 0 \\ & & \nearrow S_0 & & \nearrow S_1 & & \nearrow S_{n-1} \\ 0 & \longrightarrow & \mathcal{V}_1 \otimes \tilde{\mathbb{E}}_0 & \xrightarrow{\tilde{d}_0} & \mathcal{V}_2 \otimes \tilde{\mathbb{E}}_1 & \xrightarrow{\tilde{d}_1} & \cdots \xrightarrow{\tilde{d}_{n-1}} \mathcal{V}_{n+1} \otimes \tilde{\mathbb{E}}_n \longrightarrow 0, \end{array}$$

in which $s_i : \tilde{\mathbb{E}}_i \rightarrow \mathbb{E}_{i+1}$ is a linear operator between finite-dimensional spaces. The operators in (10) satisfy anti-commutativity: $S_{i+1}\tilde{d}_i = -d_{i+1}S_i$, and J-injectivity/surjectivity condition: for some particular J with $0 \leq J < n$, s_i is injective for $i = 0, \dots, J$ and is surjective for $i = J, \dots, n-1$. The output complex is

$$0 \rightarrow \mathcal{Y}_0 \xrightarrow{\mathcal{D}_0} \mathcal{Y}_1 \xrightarrow{\mathcal{D}_1} \cdots \xrightarrow{\mathcal{D}_{J-1}} \mathcal{Y}_J \xrightarrow{\mathcal{D}_J} \mathcal{Y}_{J+1} \xrightarrow{\mathcal{D}_{J+1}} \cdots \xrightarrow{\mathcal{D}_{n-1}} \mathcal{Y}_n \rightarrow 0,$$

where \mathcal{Y}_i is $\mathcal{V}_i \otimes (\mathbb{E}_i / \text{img}(s_{i-1}))$ for $i = 0, \dots, J$ and $\mathcal{V}_{i+1} \otimes \ker(s_i)$ for $i = J+1, \dots, n$, \mathcal{D}_i is the projection of d_i onto \mathcal{Y}_{i+1} for $i = 0, \dots, J-1$, \tilde{d}_i for $i = J+1, \dots, n-1$ and $\tilde{d}_J(S_J)^{-1}d_J$ for $i = J$. By the BGG framework, many new complexes can be generated from old ones.

In two dimensions, the de Rham complexes will form a BGG diagram

$$(11) \quad \begin{array}{ccccccc} \mathbb{R} & \xrightarrow{\subset} & H^2(\Omega) & \xrightarrow{\text{curl}} & \mathbf{H}^1(\Omega; \mathbb{R}^2) & \xrightarrow{\text{div}} & L^2(\Omega) \longrightarrow 0 \\ & & \nearrow \text{id} & & \nearrow -2 \text{sskw} & & \\ \mathbb{R}^2 & \xrightarrow{\subset} & \mathbf{H}^1(\Omega; \mathbb{R}^2) & \xrightarrow{\text{curl}} & \mathbf{L}^2(\Omega; \mathbb{M}) & \xrightarrow{\text{div}} & \mathbf{H}^{-1}(\Omega; \mathbb{R}^2) \longrightarrow 0 \\ & & \nearrow \text{mskw} & & \nearrow \text{id} & & \\ \mathbb{R} & \xrightarrow{\subset} & L^2(\Omega) & \xrightarrow{\text{curl}} & \mathbf{H}^{-1}(\Omega; \mathbb{R}^2) & \xrightarrow{\text{div}} & H^{-2}(\Omega) \longrightarrow 0 \end{array}$$

which will lead to the elasticity complex

$$\mathbb{P}_1 \xrightarrow{\subset} H^2(\Omega) \xrightarrow{\text{Air}} \mathbf{H}(\text{div}, \Omega; \mathbb{S}) \xrightarrow{\text{div}} \mathbf{L}^2(\Omega; \mathbb{R}^2) \rightarrow \mathbf{0},$$

and the divdiv complex

$$\mathbf{RT} \xrightarrow{\subset} \mathbf{H}^1(\Omega; \mathbb{R}^2) \xrightarrow{\text{sym curl}} \mathbf{H}(\text{divdiv}, \Omega; \mathbb{S}) \xrightarrow{\text{divdiv}} L^2(\Omega) \rightarrow 0.$$

By rotation, we also have the Hessian complex

$$\mathbb{P}_1 \xrightarrow{\subset} H^2(\Omega) \xrightarrow{\text{hess}} \mathbf{H}(\text{rot}, \Omega; \mathbb{S}) \xrightarrow{\text{rot}} \mathbf{L}^2(\Omega; \mathbb{R}^2) \rightarrow \mathbf{0}$$

and the strain complex

$$\mathbf{RM} \xrightarrow{\subset} \mathbf{H}^1(\Omega; \mathbb{R}^2) \xrightarrow{\text{sym grad}} \mathbf{H}(\text{rotrot}, \Omega; \mathbb{S}) \xrightarrow{\text{rotrot}} L^2(\Omega) \rightarrow 0.$$

We shall construct finite element counterpart of BGG diagram (11) and derive several finite element elasticity and divdiv complexes.

3. SMOOTH FINITE ELEMENTS IN TWO DIMENSIONS

In this section, we shall construct C^m -continuous finite elements on two-dimensional triangular grids, firstly constructed by Bramble and Zlámal [10], by a decomposition of the simplicial lattice. We start from a Hermite finite element space which ensures the tangential derivatives across edges are continuous. By adding degrees of freedom on the normal derivative, we can impose the continuity of derivatives across triangles.

We use a pair of integers $\mathbf{r} = (r^v, r^e)$ for the smoothness at vertices and at edges, respectively. To be C^m -continuous, $r^e = m$ is the minimum requirement for edges and $r^v \geq \max\{2r^e, -1\}$ for vertices. Here value -1 means no continuity. The polynomial degree $k \geq \max\{2r^v + 1, 0\}$.

3.1. Simplicial lattice. We first introduce the simplicial lattice for 2D triangle. Generalization to arbitrary dimension can be found in our recent work [18].

For two non-negative integers $l \leq m$, we will use the multi-index notation $\alpha \in \mathbb{N}^{l:m}$, meaning $\alpha = (\alpha_l, \dots, \alpha_m)$ with integer $\alpha_i \geq 0$. The length of a multi-index is $|\alpha| := \sum_{i=l}^m \alpha_i$ for $\alpha \in \mathbb{N}^{l:m}$ and $\alpha! := \alpha_l! \cdots \alpha_m!$. We can also treat α as a vector with integer-valued coordinates. Denote

$$D^\beta = \frac{\partial^{|\beta|}}{\partial x_1^{\beta_1} \partial x_2^{\beta_2}}, \quad \beta \in \mathbb{N}^{1:2}.$$

A simplicial lattice of degree k in two dimensions is a multi-index set of 3 components and with fixed length k , i.e.,

$$\mathbb{T}_k^2 = \{\alpha = (\alpha_0, \alpha_1, \alpha_2) \in \mathbb{N}^{0:2} \mid |\alpha| = k\}.$$

An element $\alpha \in \mathbb{T}_k^2$ is called a node of the lattice. We use the convention that: for a vector $\alpha \geq c$ means $\alpha_i \geq c$ for all components $i = 0, 1, 2$. It holds that

$$|\mathbb{T}_k^2| = \binom{k+2}{k} = \dim \mathbb{P}_k(T).$$

Let T be a triangle with vertices $\{v_0, v_1, v_2\}$ and $\lambda_i, i = 0, 1, 2$, be the barycentric coordinate. The Bernstein basis of $\mathbb{P}_k(T)$ is

$$\{\lambda^\alpha := \lambda_0^{\alpha_0} \lambda_1^{\alpha_1} \lambda_2^{\alpha_2} \mid \alpha \in \mathbb{T}_k^2\}.$$

For a subset $S \subseteq \mathbb{T}_k^2$, we define

$$\mathbb{P}_k(S) = \text{span}\{\lambda^\alpha, \alpha \in S \subseteq \mathbb{T}_k^2\}.$$

With such one-to-one mapping between the lattice node α and the Bernstein polynomial λ^α , we can study properties of polynomials through the simplicial lattice.

We can embed the simplicial lattice into a geometric simplex. Given $\alpha \in \mathbb{T}_k^2$, the barycentric coordinate of α is given by $\lambda(\alpha) = (\alpha_0, \alpha_1, \alpha_2)/k$, and the geometric embedding is

$$x : \mathbb{T}_k^2 \rightarrow T, \quad x(\alpha) = \sum_{i=0}^2 \lambda_i(\alpha) v_i.$$

We will always assume such a geometric embedding of the simplicial lattice exists and write as $\mathbb{T}_k^2(T)$. See Fig. 1 for an illustration for a two-dimensional simplicial lattice embedded into a triangle.

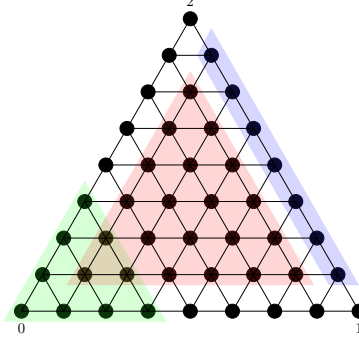


FIGURE 1. A simplicial lattice in two dimensions.

A simplicial lattice \mathbb{T}_k^2 is, by definition, an algebraic set. Through the geometric embedding $\mathbb{T}_k^2(T)$, we can use operators for the geometric simplex T to study this algebraic set. For example, for a subset $S \subseteq T$, we use $\mathbb{T}_k^2(S) = \{\alpha \in \mathbb{T}_k^2, x(\alpha) \in S\}$ to denote the portion of lattice nodes whose geometric embedding is inside S .

Following [6], we let $\Delta(T)$ denote all the sub-simplices of T , while $\Delta_\ell(T)$ denotes the set of sub-simplices of dimension ℓ , for $0 \leq \ell \leq 2$. For a sub-simplex $f \in \Delta_\ell(T)$, we will overload the notation f for both the geometric simplex and the algebraic set of indices. Namely $f = \{f(0), \dots, f(\ell)\} \subseteq \{0, 1, 2\}$ and also

$$f = \text{Convex}(v_{f(0)}, \dots, v_{f(\ell)}) \in \Delta_\ell(T)$$

is the ℓ -dimensional simplex spanned by the vertices $v_{f(0)}, \dots, v_{f(\ell)}$. If $f \in \Delta_\ell(T)$, then $f^* \in \Delta_{2-\ell-1}(T)$ denotes the sub-simplex of T opposite to f . When treating f as a subset of $\{0, 1, 2\}$, $f^* \subseteq \{0, 1, 2\}$ so that $f \cup f^* = \{0, 1, 2\}$, i.e., f^* is the complementary set of f . Geometrically,

$$f^* = \text{Convex}(v_{f^*(1)}, \dots, v_{f^*(2-\ell)}) \in \Delta_{1-\ell}(T)$$

is the $(1 - \ell)$ -dimensional simplex spanned by vertices not contained in f . Given a sub-simplex $f \in \Delta_\ell(T)$, through the geometric embedding $f \hookrightarrow T$, we define the prolongation/extension operator $E : \mathbb{T}_k^\ell(f) \rightarrow \mathbb{T}_k^2(T)$ as follows:

$$E(\alpha)_{f(i)} = \alpha_i, i = 0, \dots, \ell, \quad \text{and } E(\alpha)_j = 0, j \notin f.$$

For example, assume $f = \{1, 2\}$, then for $\alpha = (\alpha_0, \alpha_1) \in \mathbb{T}_k^1(f)$, the extension $E(\alpha) = (0, \alpha_0, \alpha_1) \in \mathbb{T}_k^2(T)$. The geometric embedding $x(E(\alpha)) \in f$ which justifies the notation $\mathbb{T}_k^\ell(f)$. With a slight abuse of notation, for a node $\alpha_f \in \mathbb{T}_k^\ell(f)$, we still use the same notation $\alpha_f \in \mathbb{T}_k^2(T)$ to denote such extension. Then we have the following direct decomposition

$$(12) \quad \alpha = E(\alpha_f) + E(\alpha_{f^*}) = \alpha_f + \alpha_{f^*}, \text{ and } |\alpha| = |\alpha_f| + |\alpha_{f^*}|.$$

Based on (12), we can write a Bernstein polynomial as

$$\lambda^\alpha = \lambda_f^{\alpha_f} \lambda_{f^*}^{\alpha_{f^*}},$$

where $\lambda_f = \lambda_{f(0)} \dots \lambda_{f(\ell)} \in \mathbb{P}_{\ell+1}(f)$ is the bubble function on f and also denoted by b_f .

The interior lattice is related to the so-called bubble polynomial of f :

$$b_f \mathbb{P}_{k-(\ell+1)}(f) := \text{span}\{b_f \lambda_f^{\alpha_f} : \alpha_f \in \mathbb{T}_{k-(\ell+1)}^\ell(f)\}.$$

Geometrically as the bubble polynomial space vanished on the boundary, it is generated by the interior lattice nodes only. In Fig. 1, $\mathbb{T}_k^2(\overset{\circ}{T})$ consists of the nodes inside the red triangle, and $\mathbb{T}_k^1(\overset{\circ}{f})$ for $f = \{1, 2\}$ is in the blue trapezoid region.

3.2. Derivative and distance. Given $f \in \Delta_\ell(T)$, we define the distance of a node $\alpha \in \mathbb{T}_k^2$ to f as

$$\text{dist}(\alpha, f) := |\alpha_{f^*}| = \sum_{i \in f^*} \alpha_i.$$

Next we present a geometric interpretation of $\text{dist}(\alpha, f)$. We set the vertex $\vee_{f(0)}$ as the origin and embed the lattice to the scaled reference simplex $k\hat{T}$ with vertices $(0, 0)$, $(k, 0)$, and $(0, k)$. Then $|\alpha_{f^*}| = s$ corresponds to the linear equation

$$x_{f^*(1)} + \dots + x_{f^*(2-\ell)} = s,$$

which defines a line in \mathbb{R}^2 , denoted by $L(f, s)$, with a normal vector $\mathbf{1}_{f^*}$. Obviously $\mathbf{1}_{f^*} \cdot e_{f(0)f(i)} = 0$ as the zero pattern is complementary to each other. So f is parallel to the line $L(f, s)$. The distance $\text{dist}(\alpha, f)$ for $\alpha \in L(f, s)$ is the intercept of the line $L(f, s)$; see Fig. 2 for an illustration. In particular $f \in L(f, 0)$ and $\lambda_i|_f = 0$ for $i \in f^*$. Indeed $f = \{x \in T \mid \lambda_i(x) = 0, i \in f^*\}$.

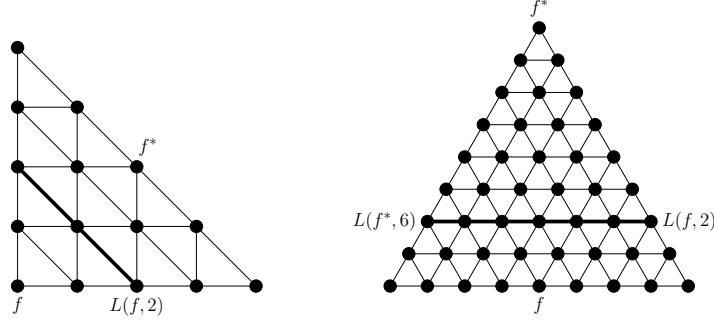


FIGURE 2. Distance to a vertex and to an edge.

We define the lattice tube of f with radius r as

$$D(f, r) = \{\alpha \in \mathbb{T}_k^2, \text{dist}(\alpha, f) \leq r\},$$

which contains lattice nodes at most r distance away from f . We overload the notation

$$L(f, s) = \{\alpha \in \mathbb{T}_k^2, \text{dist}(\alpha, f) = s\},$$

which is defined as a line before but here is a subset of lattice nodes on this line. Then by definition,

$$D(f, r) = \cup_{s=0}^r L(f, s), \quad L(f, s) = L(f^*, k - s).$$

We have the following characterization of lattice nodes in $D(f, r)$.

Lemma 3.1. For lattice node $\alpha \in \mathbb{T}_k^2$,

$$\begin{aligned}\alpha \in D(f, r) &\iff |\alpha_{f^*}| \leq r \iff |\alpha_f| \geq k - r, \\ \alpha \notin D(f, r) &\iff |\alpha_{f^*}| > r \iff |\alpha_f| \leq k - r - 1.\end{aligned}$$

Proof. By definition of $\text{dist}(\alpha, f)$ and the fact $|\alpha_f| + |\alpha_{f^*}| = k$. \square

For each vertex $v_i \in \Delta_0(T)$,

$$D(v_i, r) = \{\alpha \in \mathbb{T}_k^2, |\alpha_{i^*}| \leq r\},$$

which is isomorphic to a simplicial lattice \mathbb{T}_r^2 of degree r ; see the green triangle in Fig. 1. For an edge $e \in \Delta_1(T)$, $D(e, r)$ is a trapezoid of height r with base e .

Recall that in [6] a smooth function u is said to vanish to order r on f if $D^\beta u|_f = 0$ for all $\beta \in \mathbb{N}^{1:2}$, $|\beta| < r$. The following result shows that the vanishing order r of a Bernstein polynomial λ^α on f is the distance $\text{dist}(\alpha, f)$.

Lemma 3.2. Let $f \in \Delta_\ell(T)$ be a sub-simplex of T . For $\alpha \in \mathbb{T}_k^2$, $\beta \in \mathbb{N}^{1:2}$, and $|\alpha_{f^*}| > |\beta|$, i.e., $\text{dist}(\alpha, f) > |\beta|$, then

$$D^\beta \lambda^\alpha|_f = 0.$$

Proof. For $\alpha \in \mathbb{T}_k^2$, we write $\lambda^\alpha = \lambda_f^{\alpha_f} \lambda_{f^*}^{\alpha_{f^*}}$. When $|\alpha_{f^*}| > |\beta|$, the derivative $D^\beta \lambda^\alpha$ will contain a factor $\lambda_{f^*}^\gamma$ with $\gamma \in \mathbb{N}^{1:(2-\ell)}$, and $|\gamma| = |\alpha_{f^*}| - |\beta| > 0$. Therefore $D^\beta \lambda^\alpha|_f = 0$ as $\lambda_i|_f = 0$ for $i \in f^*$. \square

3.3. Derivatives at vertices. Consider a function $u \in C^m(\Omega)$. The set of derivatives of order up to m can be written as

$$\{D^\alpha u, \alpha \in \mathbb{N}^{1:2}, |\alpha| \leq m\}.$$

Notice that the multi-index $\alpha \in \mathbb{N}^{1:2}$. We can add component $\alpha_0 = m - |\alpha|$. Then the index set forms a simplicial lattice \mathbb{T}_m^2 of degree m . For each vertex, we can use the small simplicial lattice $\mathbb{T}_m^2 \cong D(v_i, m)$ to determine the derivatives at that vertex; see the green triangle in Fig. 3 (a) and (b).

Lemma 3.3. Let $i \in \{0, 1, 2\}$. The polynomial space

$$\mathbb{P}_k(D(v_i, m)) := \text{span} \{\lambda^\alpha, \alpha \in \mathbb{T}_k^2, \text{dist}(\alpha, v_i) = |\alpha_{i^*}| \leq m\},$$

is uniquely determined by the DoFs

$$(13) \quad \{D^\beta u(v_i), \beta \in \mathbb{N}^{1:2}, |\beta| \leq m\}.$$

Proof. Obviously the dimensions match. Indeed, a one-to-one mapping is from α_{i^*} to β . So it suffices to show that for $u \in \mathbb{P}_k(D(v_i, m))$ if DoF (13) vanishes, then $u = 0$.

Without loss of generality, we assume $i = 0$. Clearly $\{\nabla \lambda_1, \nabla \lambda_2\}$ forms a basis of \mathbb{R}^2 . We choose another basis $\{l^1, l^2\}$ of \mathbb{R}^2 , being dual to $\{\nabla \lambda_1, \nabla \lambda_2\}$, i.e., $\nabla \lambda_i \cdot l^j = \delta_{i,j}$. Indeed l^i is the edge vector e_{0i} . We can express the derivatives in this non-orthogonal basis and denote by $D_n^\beta u := \frac{\partial^{|\beta|} u}{\partial (l^1)^{\beta_1} \partial (l^2)^{\beta_2}}$.

It is easy to show that, for each $r = 0, 1, \dots, m$, vanishing $\{D_n^\beta u, \beta \in \mathbb{N}^{1:2}, |\beta| = r\}$ is equivalent to the vanishing $\{D^\beta u, \beta \in \mathbb{N}^{1:2}, |\beta| = r\}$. By the duality $\nabla \lambda_i \cdot l^j = \delta_{i,j}$, $i, j = 1, 2$,

$$(14) \quad D_n^\beta(\lambda_0^\alpha) = \beta! \delta(\alpha, \beta) \quad \text{for } \alpha, \beta \in \mathbb{N}^{1:2}, |\alpha| = |\beta| = r,$$

where $\beta! = \beta_1! \beta_2!$ and $\delta(\alpha, \beta)$ is the Kronecker delta function. When T is the reference triangle, $\lambda_0^\alpha = x_1^{\alpha_1} x_2^{\alpha_2}$, $D_n^\beta = D^\beta$, and (14) is the standard calculus result.

A basis of $\mathbb{P}_k(D(v_0, m))$ is given by $\{\lambda_0^{k-|\alpha|}\lambda_{0^*}^\alpha, \alpha \in \mathbb{N}^{1:2}, |\alpha| \leq m\}$. Assume $u = \sum_{\substack{\alpha \in \mathbb{N}^{1:2} \\ |\alpha| \leq m}} c_\alpha \lambda_0^{k-|\alpha|}\lambda_{0^*}^\alpha$ with $c_\alpha \in \mathbb{R}$ and $D^\beta u(v_0) = 0$ for all $\beta \in \mathbb{N}^{1:2}$ satisfying $|\beta| \leq m$.

We prove $c_\alpha = 0$ by induction of $|\alpha|$.

When $|\alpha| = 0$, as $u(v_0) = c_{(0,0)}$ and $u(v_0) = 0$, we conclude $c_{(0,0)} = 0$. Assume $c_\alpha = 0$ for all $\alpha \in \mathbb{N}^{1:2}$ satisfying $|\alpha| \leq r-1$, i.e., $u = \sum_{\substack{\alpha \in \mathbb{N}^{1:2} \\ r \leq |\alpha| \leq m}} c_\alpha \lambda_0^{k-|\alpha|}\lambda_{0^*}^\alpha$.

By Lemma 3.2, the derivative $D^\beta(\lambda_0^{k-|\alpha|}\lambda_{0^*}^\alpha)$ vanishes at v_0 for all $\beta \in \mathbb{N}^{1:2}$ satisfying $|\beta| < |\alpha|$. Hence, for $|\beta| = r$, using (14),

$$D_n^\beta u(v_0) = D_n^\beta \left(\sum_{\alpha \in \mathbb{N}^{1:2}, |\alpha|=r} c_\alpha \lambda_0^{k-r}\lambda_{0^*}^\alpha \right) (v_0) = \beta! c_\beta = 0,$$

which implies $c_\beta = 0$ for all $\beta \in \mathbb{N}^{1:2}, |\beta| = r$. Induction for $r = 1, 2, \dots, m$ to conclude $u = 0$. \square

Here is a summary of the proof. The DoF-Function matrix $(D_n^\beta(\lambda_0^{k-|\alpha|}\lambda_{0^*}^\alpha)(v_0))_{\beta, \alpha}$ is block lower triangular where the lattice nodes are sorted by their length. Then if each block matrix on the diagonal ($|\alpha| = |\beta| = r$) is invertible, the whole matrix is invertible which is equivalent to the unisolvence. For the block diagonal matrix, we switch to the derivative D_n^β which is dual to the Bernstein form of polynomials.

3.4. Normal derivatives on edges. Given an edge e , we first identify lattice nodes to determine the normal derivative

$$\left\{ \frac{\partial^\beta u}{\partial n_e^\beta} \Big|_e, 0 \leq \beta \leq m \right\}.$$

By Lemma 3.2, if the lattice node is $r^e + 1$ away from the edge, then the corresponding Bernstein polynomial will have vanishing normal derivatives up to order r^e .

On the two vertices, we have used $D(\Delta_0(e), r^v)$ for the derivative at vertices. So we will use the rest, i.e., $D(e, r^e) \setminus D(\Delta_0(e), r^v)$ for the normal derivative.

Lemma 3.4. *Let $r^v \geq r^e \geq 0$ and $k \geq 2r^v + 1$. Let $e \in \Delta_1(T)$ be an edge of a triangle T . The polynomial function space $\mathbb{P}_k(D(e, r^e) \setminus D(\Delta_0(e), r^v))$ is determined by DoFs*

$$\int_e \frac{\partial^\beta u}{\partial n_e^\beta} \lambda_e^{\alpha_e} ds \quad \alpha_e \in \mathbb{T}_{k-2(r^v+1)+\beta}^1, \beta = 0, 1, \dots, r^e.$$

Proof. Without loss of generality, we take $e = e_{0,1}$. By definition $D(e, r^e) = \bigoplus_{i=0}^{r^e} L(e, i)$, where recall that

$$L(e, i) = \{\alpha \in \mathbb{T}_k^2, \text{dist}(\alpha, e) = i\} = \{\alpha \in \mathbb{T}_k^2, \alpha_2 = i\} = \{\alpha \in \mathbb{T}_k^2, \alpha_0 + \alpha_1 = k - i\}$$

consists of lattice nodes parallel to e and with distance i . Then $L(e, i) \cong \mathbb{T}_{k-i}^1(e)$ by keeping (α_0, α_1) only.

Now we use the requirement $\alpha \notin D(\Delta_0(e), r^v)$ to figure out the range of the nodes. Using Lemma 3.1, we derive from $\text{dist}(\alpha, v_0) > r^v$ that $\alpha_0 < k - r^v$. Together with $\alpha_0 + \alpha_1 = k - i$, we get the lower bound $\alpha_1 \geq r^v - i + 1$. Similarly $\alpha_0 \geq r^v - i + 1$. Therefore the line segment

$$L(e, i) \setminus D(\Delta_0(e), r^v) = \{(\alpha_0, \alpha_1, i), \alpha_0 + \alpha_1 = k - i, \min\{\alpha_0, \alpha_1\} \geq r^v - i + 1\},$$

which can be identified with the lattice $\mathbb{T}_{k-2(r^v+1)+i}^1$ without inequality constraint.

Applying the same argument in the proof of Lemma 3.3, it follows from Lemma 3.2 that matrix $(\frac{\partial^\beta}{\partial n_e^\beta}(\lambda_e^{\alpha_e} \lambda_2^i)|_e)_{\beta,i}$ is lower block triangular. Hence it suffices to prove the polynomial function space $\mathbb{P}_k(L(e, i) \setminus D(\Delta_0(e), r^\vee))$ is determined by DoFs

$$(15) \quad \int_e \frac{\partial^i u}{\partial n_e^i} \lambda_e^{\alpha_e} ds \quad \alpha_e \in \mathbb{T}_{k-2(r^\vee+1)+i}^1.$$

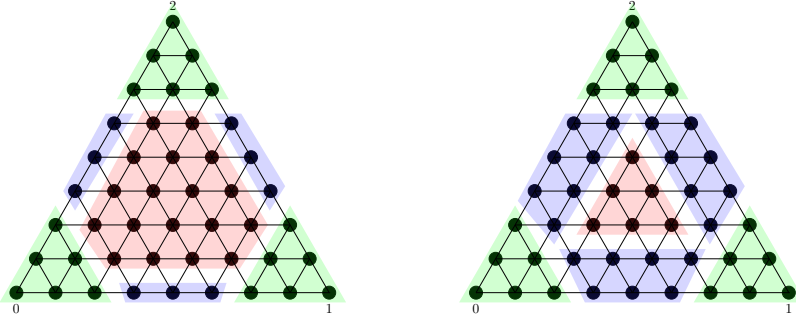
Take a $u = \sum_{\alpha_e \in \mathbb{T}_{k-2(r^\vee+1)+i}^1} c_{\alpha_e} \lambda_e^{\alpha_e} \lambda_e^{r^\vee-i+1} \lambda_2^i \in \mathbb{P}_k(L(e, i) \setminus D(\Delta_0(e), r^\vee))$ with coefficients $c_{\alpha_e} \in \mathbb{R}$. Then

$$\frac{\partial^i u}{\partial n_e^i} \Big|_e = i!(n_e \cdot \nabla \lambda_2)^i \lambda_e^{r^\vee-i+1} \sum_{\alpha_e \in \mathbb{T}_{k-2(r^\vee+1)+i}^1} c_{\alpha_e} \lambda_e^{\alpha_e}.$$

Noting that $n_e \cdot \nabla \lambda_2$ is a constant and λ_e is always positive in the interior of e , the vanishing DoF (15) means $c_{\alpha_e} = 0$ for all $\alpha_e \in \mathbb{T}_{k-2(r^\vee+1)+i}^1$. Consequently $u = 0$. \square

Geometrically we push all lattice nodes in $D(e, r^e) \setminus D(\Delta_0(e), r^\vee)$ to the edge to determine normal derivatives on e up to order r^e .

3.5. Geometric decompositions of the simplicial lattice. The requirement $r^e \leq r^\vee$ in Lemma 3.4 is due to the fact that the smoothness of the normal derivative is less than or equal to that of the vertices. Inside a triangle, a vertex will be shared by two edges and to have enough lattice nodes for each edge, $r^\vee \geq 2r^e$ is required.



(a) The geometric decomposition of a Hermite element.

(b) The geometric decomposition of a C^1 element: $m = 1, r^e = 1, r^\vee = 2, k = 8$.

FIGURE 3. Comparison of the geometric decompositions of a two-dimensional Hermite element and a C^1 -conforming element.

Lemma 3.5. *Let $r^e = m \geq -1$, $r^\vee \geq \max\{2r^e, -1\}$, and nonnegative integer $k \geq 2r^\vee + 1 \geq 4m + 1$. Let T be a triangle. Then it holds that*

$$(16) \quad \mathbb{T}_k^2(T) = S_0(T) \oplus S_1(T) \oplus S_2(T),$$

where

$$\begin{aligned} S_0(T) &= D(\Delta_0(T), r^\vee), \\ S_1(T) &= \bigoplus_{e \in \Delta_1(T)} (D(e, r^e) \setminus S_0(T)), \\ S_2(T) &= \mathbb{T}_k^2(T) \setminus (S_0(T) \oplus S_1(T)), \end{aligned}$$

with cardinality

$$\begin{aligned} |S_0(T)| &= 3 \binom{r^\vee + 2}{2}, \\ |S_1(T)| &= 3 \sum_{i=0}^{r^e} (k - 1 - 2r^\vee + i), \\ |S_2(T)| &= \binom{k + 2}{2} - |S_0(T)| - |S_1(T)|. \end{aligned}$$

This leads to the decomposition of the polynomial space

$$(17) \quad \mathbb{P}_k(T) = \mathbb{P}_k(S_0(T)) \oplus \mathbb{P}_k(S_1(T)) \oplus \mathbb{P}_k(S_2(T)).$$

Furthermore, we have characterization

$$(18) \quad \mathbb{P}_k(S_1(T)) = \bigoplus_{e \in \Delta_1(T)} \bigoplus_{i=0}^m b_T^i b_e^{r^\vee + 1 - 2i} \mathbb{P}_{k - 2(r^\vee + 1) + i}(e),$$

and

$$(19) \quad \mathbb{P}_k(S_2(T)) = b_T^{r^e + 1} \overset{\circ}{\mathbb{P}}_{k - 3(r^e + 1)}(\mathbf{r}),$$

where

$$(20) \quad \overset{\circ}{\mathbb{P}}_{k - 3(r^e + 1)}(\mathbf{r}) = \text{span}\{\lambda^\alpha, \alpha \in \mathbb{T}_{k - 3(r^e + 1)}^2, \alpha \leq k - r^\vee - r^e - 2\}.$$

Proof. As $k \geq 2r^\vee + 1$, the sets $\{D(\vee, r^\vee), \vee \in \Delta_0(T)\}$ are disjoint.

We then show that the sets $\{D(e, r^e) \setminus D(\Delta_0(e), r^\vee), e \in \Delta_1(T)\}$ are disjoint. A node $\alpha \in D(e_{01}, r^e)$ implies $\alpha_2 \leq r^e$ and $\alpha \in D(e_{02}, r^e)$ implies $\alpha_1 \leq r^e$. Therefore $|\alpha_{0^*}| = \alpha_1 + \alpha_2 \leq 2r^e \leq r^\vee$, i.e., $(D(e_{01}, r^e) \cap D(e_{02}, r^e)) \subseteq D(\vee_0, r^\vee)$. Repeat the argument for each pair of edges to conclude $\{D(e, r^e) \setminus D(\Delta_0(e), r^\vee), e \in \Delta_1(T)\}$ are disjoint.

For a given edge e , e^* is the vertex opposite to e and $L(e^*, r^\vee) = L(e, k - r^\vee)$. As $k - r^\vee > r^e$, we conclude $D(e, r^e) \cap D(e^*, r^\vee) = \emptyset$ and consequently $D(e, r^e) \setminus D(\Delta_0(T), r^\vee) = D(e, r^e) \setminus D(\Delta_0(e), r^\vee)$.

Then decompositions (16) and (17) follow.

To show (18), we notice that, for a lattice node $\alpha \in D(e_{01}, r^e) \setminus D(\Delta_0(e_{01}), r^\vee)$, it satisfies the constraint

$$\alpha_2 \leq r^e, \alpha_0 + \alpha_2 > r^\vee, \alpha_1 + \alpha_2 > r^\vee, \alpha_0 + \alpha_1 + \alpha_2 = k.$$

We let $\alpha_2 = i$ for $i = 0, 1, \dots, r^e = m$. Then

$$\lambda_0^{\alpha_0} \lambda_1^{\alpha_1} \lambda_2^{\alpha_2} = \lambda^i (\lambda_0 \lambda_1)^{r^\vee - 2i + 1} \lambda_0^{\alpha_0 - (r^\vee + 1) + i} \lambda_1^{\alpha_1 - (r^\vee + 1) + i} = b_T^i b_e^{r^\vee - 2i + 1} \lambda_e^{\alpha_e}$$

with $\alpha_e \in \mathbb{T}_{k - 2(r^\vee + 1) + i}^{0:1}$, which gives (18). For a node $\alpha \in S_2(T)$, it satisfies the constraint

$$\alpha_0 + \alpha_1 + \alpha_2 = k, \alpha > r^e, \alpha < k - r^\vee.$$

Then set $\tilde{\alpha} = \alpha - (r^e + 1)$. We can write

$$\lambda^\alpha = \lambda^{r^e + 1} \lambda^{\tilde{\alpha}}, |\tilde{\alpha}| = k - 3(r^e + 1), \tilde{\alpha} \leq k - r^\vee - r^e - 2,$$

which leads to (19).

The cardinalities $|S_0|$ and $|S_2|$ are straight forward and $|S_1|$ is given by (18). \square

Denote by

$$\mathbb{B}_k(\mathbf{r}) = \mathbb{B}_k(\mathbf{r}; T) := \mathbb{P}_k(S_2(T)) = \text{span}\{\lambda^\alpha, \alpha \in S_2(T)\},$$

and call it polynomial bubble space, which will play an important role in our construction of finite element de Rham complexes.

3.6. Smooth finite elements in two dimensions.

Theorem 3.6. *Let $r^e = m \geq -1$, $r^v \geq \max\{2r^e, -1\}$, and nonnegative integer $k \geq 2r^v + 1$. Let T be a triangle. The shape function space $\mathbb{P}_k(T)$ is determined by the DoFs*

$$(21) \quad D^\alpha u(v) \quad \alpha \in \mathbb{N}^{1:2}, |\alpha| \leq r^v, v \in \Delta_0(T),$$

$$(22) \quad \int_e \frac{\partial^\beta u}{\partial n_e^\beta} q \, ds \quad q \in \mathbb{P}_{k-2(r^v+1)+\beta}(e), \beta = 0, 1, \dots, r^e,$$

$$(23) \quad \int_T u q \, dx \quad q \in \mathbb{B}_k(\mathbf{r}).$$

Proof. By the decomposition (17) of $\mathbb{P}_k(T)$ and characterization (18)-(19), the dimension of $\mathbb{P}_k(T)$ matches the number of DoFs. Let $u \in \mathbb{P}_k(T)$ satisfy all the DoFs (21)-(23) vanish. Thanks to Lemma 3.3, Lemma 3.4 and Lemma 3.5, it follows from the vanishing DoFs (21) and (22) that $u \in \mathbb{P}_k(S_2(T))$. Then $u = 0$ holds from the vanishing DoF (23). \square

When $r^e = m = 1$ and $r^v = 2$, this is known as Argyris element [1, 30]. When $r^e = m$, $r^v = 2m$ and $k = 4m + 1$, C^m -continuous finite elements are constructed in [10, 32], see also [28, Section 8.1] and the references therein, whose DoFs are different from (23). Ours are similar to DoFs constructed in [25]. As b_T is always positive in the interior of T , in DoF (23), it can be further changed to $q \in \mathring{\mathbb{P}}_{k-3(r^e+1)}(\mathbf{r})$.

With mesh \mathcal{T}_h , define the global C^m -continuous finite element space

$$V(\mathcal{T}_h) = \{u \in C^m(\Omega) : u|_T \in \mathbb{P}_k(T) \text{ for all } T \in \mathcal{T}_h, \\ \text{and all the DoFs (21) and (22) are single-valued}\}.$$

Then $V(\mathcal{T}_h)$ admits the following geometric decomposition

$$V(\mathcal{T}_h) = \bigoplus_{v \in \Delta_0(\mathcal{T}_h)} \mathbb{P}_k(D(v, r^v)) \oplus \bigoplus_{e \in \Delta_1(\mathcal{T}_h)} \mathbb{P}_k(D(e, r^e) \setminus D(\Delta_0(e), r^v)) \\ \oplus \bigoplus_{T \in \mathcal{T}_h} \mathbb{B}_k(\mathbf{r}, T).$$

The dimension of $V(\mathcal{T}_h)$ is

$$\dim V(\mathcal{T}_h) = |\Delta_0(\mathcal{T}_h)| \binom{r^v + 2}{2} + |\Delta_1(\mathcal{T}_h)| \left[\binom{k - 2r^v + r^e}{2} - \binom{k - 2r^v - 1}{2} \right] \\ + |\Delta_2(\mathcal{T}_h)| \left[\binom{k - 3r^e - 1}{2} - 3 \binom{r^v - 2r^e}{2} \right].$$

Denoted by $\tilde{k} = k - 3(r^e + 1)$ and $\tilde{r} = r^v - 2r^e - 2$. By Lemma 3.1, we can view the constraint in (20) as $\alpha \notin D(v_i, \tilde{r})$ and thus obtain another formula on the dimension

$$\dim \mathbb{B}_k(\mathbf{r}) = \binom{\tilde{k} + 2}{2} - 3 \binom{\tilde{r} + 2}{2} = \binom{k - 3r^e - 1}{2} - 3 \binom{r^v - 2r^e}{2}.$$

In particular, for the minimum degree case: $r^e = m, r^v = 2m, k = 4m + 1$ with $m \geq 0$, we denoted by $V^{\text{BZ}}(\mathcal{T}_h)$ and the dimension

$$\dim V^{\text{BZ}}(\mathcal{T}_h) = |\Delta_0(\mathcal{T}_h)| \binom{2m+2}{2} + |\Delta_1(\mathcal{T}_h)| \binom{m+1}{2} + |\Delta_2(\mathcal{T}_h)| \binom{m}{2}.$$

When $m = 0, 1$, there is no interior moments as $k = 4m + 1$ is not large enough.

4. FINITE ELEMENT DE RHAM COMPLEXES

In this section we shall construct finite element spaces with appropriate DoFs which make the global finite element complexes (6) exact. Unlike the classical FEEC [5], additional smoothness on lower sub-simplexes (vertices and edges for a two-dimensional triangulation) will be imposed, which are described by three vectors $\mathbf{r}_0, \mathbf{r}_1$, and \mathbf{r}_2 with the subscript referring to the i -form for $i = 0, 1, 2$. Each $\mathbf{r}_i = (r_i^v, r_i^e)$ consists of two parameters for the smoothness at vertices and edges, respectively, and $r_i^v \geq 2r_i^e$ for $i = 0, 1, 2$.

4.1. Continuous vector finite element space and decay smoothness. Relations of $\mathbf{r}_0, \mathbf{r}_1$, and \mathbf{r}_2 are needed to form the discrete de Rham complex. We first consider a simple case:

$$(24) \quad \mathbf{r}_1 \geq 0, \quad \mathbf{r}_0 = \mathbf{r}_1 + 1, \quad \mathbf{r}_2 = \mathbf{r}_1 - 1.$$

As the two-dimensional curl is a rotation of grad, we must have $\mathbf{r}_1 = \mathbf{r}_0 - 1$ but the relation $\mathbf{r}_2 = \mathbf{r}_1 - 1$ is imposed for simplicity. So the smoothness parameters are decreased by 1. The relation (24) and the requirement $r_0^v \geq 2r_0^e$ imply

$$r_1^e \geq 0, \quad r_1^v \geq 2r_1^e + 1, \quad k \geq 2r_1^v + 2.$$

For completeness, we explicitly define the finite element spaces on a conforming triangulation \mathcal{T}_h of Ω . For $k + 1 \geq 2r_0^v + 1$, the DoFs

$$(25) \quad \nabla^i v(\mathbf{v}), \quad \mathbf{v} \in \Delta_0(\mathcal{T}_h), i = 0, \dots, r_0^v,$$

$$(26) \quad \int_e \partial_n^i v q ds, \quad q \in \mathbb{P}_{k+1-2(r_0^v+1)+i}(e), e \in \Delta_1(\mathcal{T}_h), i = 0, 1, \dots, r_0^e,$$

$$\int_T v q dx, \quad q \in \mathbb{B}_{k+1}(\mathbf{r}_0), T \in \mathcal{T}_h$$

determine a $C^{r_0^e}$ -continuous finite element space

$$\mathbb{V}_{k+1}^{\text{curl}}(\mathcal{T}_h; \mathbf{r}_0) = \{v \in H^1(\Omega) : v|_T \in \mathbb{P}_{k+1}(T) \forall T \in \mathcal{T}_h, \\ \text{all the DoFs (25)-(26) are single-valued}\}.$$

For $k \geq 2r_1^v + 1$, the DoFs

$$(27) \quad \nabla^i \mathbf{v}(\mathbf{v}), \quad \mathbf{v} \in \Delta_0(\mathcal{T}_h), i = 0, \dots, r_1^v,$$

$$(28) \quad \int_e \partial_n^i \mathbf{v} \cdot \mathbf{q} ds, \quad \mathbf{q} \in \mathbb{P}_{k-2(r_1^v+1)+i}^2(e), e \in \Delta_1(\mathcal{T}_h), i = 0, 1, \dots, r_1^e,$$

$$(29) \quad \int_T \mathbf{v} \cdot \mathbf{q} dx, \quad \mathbf{q} \in \mathbb{B}_k^2(\mathbf{r}_1), T \in \mathcal{T}_h$$

determine a $C^{r_1^e}$ -continuous conforming finite element space

$$\mathbb{V}_k^{\text{div}}(\mathcal{T}_h; \mathbf{r}_1) = \{\mathbf{v} \in \mathbf{L}^2(\Omega; \mathbb{R}^2) : \mathbf{v}|_T \in \mathbb{P}_k(T; \mathbb{R}^2) \forall T \in \mathcal{T}_h, \\ \text{all the DoFs (27)-(28) are single-valued}\}.$$

For $k - 1 \geq 2r_2^v + 1$, the DoFs

$$(30) \quad \nabla^i v(\mathbf{v}), \quad \mathbf{v} \in \Delta_0(\mathcal{T}_h), i = 0, \dots, r_2^v,$$

$$(31) \quad \int_e \partial_n^i v q ds, \quad q \in \mathbb{P}_{k-1-2(r_2^v+1)+i}(e), e \in \Delta_1(\mathcal{T}_h), i = 0, 1, \dots, r_2^e,$$

$$\int_T vq dx, \quad q \in \mathbb{B}_{k-1}(\mathbf{r}_2), T \in \mathcal{T}_h$$

determine a $C^{r_2^e}$ -continuous finite element space

$$\mathbb{V}_{k-1}^{L^2}(\mathcal{T}_h; \mathbf{r}_2) = \{v \in L^2(\Omega) : v|_T \in \mathbb{P}_{k-1}(T) \forall T \in \mathcal{T}_h, \\ \text{all the DoFs (30)-(31) are single-valued}\}.$$

Lemma 4.1. *Let $r_1^e \geq 0, r_1^v \geq 2r_1^e + 1, k \geq 2r_1^v + 2$, and let $\mathbf{r}_0 = \mathbf{r}_1 + 1, \mathbf{r}_2 = \mathbf{r}_1 - 1$. Write*

$$\dim \mathbb{V}_{k+1}^{\text{curl}}(\mathcal{T}_h; \mathbf{r}_0) = C_{00}|\Delta_0(\mathcal{T}_h)| + C_{01}|\Delta_1(\mathcal{T}_h)| + C_{02}|\Delta_2(\mathcal{T}_h)|,$$

$$\dim \mathbb{V}_k^{\text{div}}(\mathcal{T}_h; \mathbf{r}_1) = C_{10}|\Delta_0(\mathcal{T}_h)| + C_{11}|\Delta_1(\mathcal{T}_h)| + C_{12}|\Delta_2(\mathcal{T}_h)|,$$

$$\dim \mathbb{V}_{k-1}^{L^2}(\mathcal{T}_h; \mathbf{r}_2) = C_{20}|\Delta_0(\mathcal{T}_h)| + C_{21}|\Delta_1(\mathcal{T}_h)| + C_{22}|\Delta_2(\mathcal{T}_h)|.$$

The coefficients C_{ij} are presented in the following table

	$ \Delta_0(\mathcal{T}_h) $	$ \Delta_1(\mathcal{T}_h) $	$ \Delta_2(\mathcal{T}_h) $
$\dim \mathbb{V}_{k+1}^{\text{curl}}(\mathcal{T}_h; \mathbf{r}_0)$	$\binom{r_0^v+2}{2}$	$\sum_{i=0}^{r_0^e} (k - 2r_0^v + i)$	$\binom{k+3}{2} - 3(C_{00} + C_{01})$
$\dim \mathbb{V}_k^{\text{div}}(\mathcal{T}_h; \mathbf{r}_1)$	$2\binom{r_1^v+2}{2}$	$2\sum_{i=0}^{r_1^e} (k - 1 - 2r_1^v + i)$	$2\binom{k+2}{2} - 3(C_{10} + C_{11})$
$\dim \mathbb{V}_{k-1}^{L^2}(\mathcal{T}_h; \mathbf{r}_2)$	$\binom{r_2^v+2}{2}$	$\sum_{i=0}^{r_2^e} (k - 2 - 2r_2^v + i)$	$\binom{k+1}{2} - 3(C_{20} + C_{21})$
$C_{0i} - C_{1i} + C_{2i}$	1	-1	1

Proof. The dimension related to $|\Delta_0(\mathcal{T}_h)|$ and $C_{00} - C_{10} + C_{20} = 1$, can be verified directly. For the column of $|\Delta_1(\mathcal{T}_h)|$, by removing the same $k - 1 - 2r_1^v$,

$$C_{01} - C_{11} + C_{21} = \sum_{i=0}^{r_0^e} (i - 1) - 2 \sum_{i=0}^{r_1^e} i + \sum_{i=0}^{r_2^e} (i + 1) = -1.$$

With these two identities, the third column is an easy consequence of (9). \square

As a corollary, we obtain the following polynomial bubble complex.

Corollary 4.2. *Let $r_1^e \geq 0, r_1^v \geq 2r_1^e + 1, k \geq 2r_1^v + 2$, and let $\mathbf{r}_0 = \mathbf{r}_1 + 1, \mathbf{r}_2 = \mathbf{r}_1 - 1$. The polynomial bubble complex*

$$(32) \quad 0 \xrightarrow{\subset} \mathbb{B}_{k+1}(\mathbf{r}_0) \xrightarrow{\text{curl}} \mathbb{B}_k^2(\mathbf{r}_1) \xrightarrow{\text{div}} \mathbb{B}_{k-1}(\mathbf{r}_2) \xrightarrow{Q_0} \mathbb{R} \rightarrow 0$$

is exact, where Q_0 is the L^2 -projection onto the constant space.

Proof. Clearly we have $\mathbb{B}_k^2(\mathbf{r}_1) \cap \ker(\operatorname{div}) = \operatorname{curl} \mathbb{B}_{k+1}(\mathbf{r}_0)$. Thanks to the last column of the table in Lemma 4.1,

$$\dim \mathbb{B}_{k+1}(\mathbf{r}_0) - \dim \mathbb{B}_k^2(\mathbf{r}_1) + \dim \mathbb{B}_{k-1}(\mathbf{r}_2) - 1 = 0,$$

which together with Lemma 2.1 concludes the exactness of bubble complex (32). \square

As a result of the bubble complex (32), when defining the space $\mathbb{V}_k^{\operatorname{div}}(\mathcal{T}_h; \mathbf{r}_1)$, by Lemma 2.1 in [16] (see also Lemma 4.10 in [15]), DoF (29) can be replaced by

$$\begin{aligned} \int_T \operatorname{div} \mathbf{v} q \, dx, \quad q \in \mathbb{B}_{k-1}(\mathbf{r}_2)/\mathbb{R}, T \in \mathcal{T}_h, \\ \int_T \mathbf{v} \cdot \operatorname{curl} q \, dx, \quad q \in \mathbb{B}_{k+1}(\mathbf{r}_0), T \in \mathcal{T}_h. \end{aligned}$$

Theorem 4.3. *Let $r_1^e \geq 0, r_1^v \geq 2r_1^e + 1, k \geq 2r_1^v + 2$, and let $\mathbf{r}_0 = \mathbf{r}_1 + 1, \mathbf{r}_2 = \mathbf{r}_1 - 1$. The finite element complex*

$$(33) \quad \mathbb{R} \xrightarrow{\subset} \mathbb{V}_{k+1}^{\operatorname{curl}}(\mathcal{T}_h; \mathbf{r}_0) \xrightarrow{\operatorname{curl}} \mathbb{V}_k^{\operatorname{div}}(\mathcal{T}_h; \mathbf{r}_1) \xrightarrow{\operatorname{div}} \mathbb{V}_{k-1}^{L^2}(\mathcal{T}_h; \mathbf{r}_2) \rightarrow 0$$

is exact.

Proof. By construction (33) is a complex, and

$$\operatorname{curl} \mathbb{V}_{k+1}^{\operatorname{curl}}(\mathcal{T}_h; \mathbf{r}_0) = \mathbb{V}_k^{\operatorname{div}}(\mathcal{T}_h; \mathbf{r}_1) \cap \ker(\operatorname{div}).$$

By Lemma 4.1 and the Euler's formula,

$$\begin{aligned} 1 - \dim \mathbb{V}_{k+1}^{\operatorname{curl}}(\mathcal{T}_h; \mathbf{r}_0) + \dim \mathbb{V}_k^{\operatorname{div}}(\mathcal{T}_h; \mathbf{r}_1) - \dim \mathbb{V}_{k-1}^{L^2}(\mathcal{T}_h; \mathbf{r}_2) \\ = 1 - |\Delta_0(\mathcal{T}_h)| + |\Delta_1(\mathcal{T}_h)| - |\Delta_2(\mathcal{T}_h)| = 0. \end{aligned}$$

Therefore the exactness of complex (33) follows from Lemma 2.1. \square

When $r_1 \geq 0$, the vector element is C^0 and can be used as the velocity space in discretization of Stokes equation.

Example 4.4. The two-dimensional finite element de Rham complexes constructed by Falk and Neilan [23] correspond to the case $r_1^e = 0, r_1^v = 1$, and $k \geq 4$:

$$\mathbb{R} \xrightarrow{\subset} \operatorname{Argy}_{k+1}\left(\begin{pmatrix} 2 \\ 1 \end{pmatrix}\right) \xrightarrow{\operatorname{curl}} \operatorname{Herm}_k\left(\begin{pmatrix} 1 \\ 0 \end{pmatrix}\right) \xrightarrow{\operatorname{div}} \mathbb{V}_{k-1}^{L^2}\left(\begin{pmatrix} 0 \\ -1 \end{pmatrix}\right) \rightarrow 0.$$

To fit the space, we skip \mathcal{T}_h in the notation and write $\mathbf{r}_i = \begin{pmatrix} r_i^v \\ r_i^e \end{pmatrix}$ as column vectors.

The vector element is C^0 and thus the previous finite element is C^1 for which the lowest degree is the Argyris element with shape function space \mathbb{P}_5 . The last one is discontinuous \mathbb{P}_3 but continuous at vertices. If we want to use a continuous element for the pressure, i.e., $\mathbf{r}_2 = (2, 0)$, then $\mathbf{r}_1 = (3, 1), \mathbf{r}_0 = (4, 2)$ and $k \geq 8$, which may find an application in the strain gradient elasticity problem [29]. Later on, we will relax the relation $\mathbf{r}_2 = \mathbf{r}_1 - 1$ and construct relative low degree Stokes pair with continuous pressure elements.

Notice that the pair $\mathbf{r}_1 = (0, 0)$ and $\mathbf{r}_2 = (-1, -1)$ are not allowed since $\mathbf{r}_0 = \mathbf{r}_1 + 1 = (1, 1)$ cannot define a C^1 element. Stability for Stokes pair $\operatorname{Lagrange}_k - \operatorname{DG}_{k-1}$ is more subtle and not covered in our framework.

4.2. Normal continuous finite elements for vector functions. We continue to consider $r_1^e = -1$ and the smoothness on edges are fixed by:

$$r_0^e = 0, \quad r_1^e = -1, \quad r_2^e = -1.$$

The constraints on the vertices smoothness are

$$r_0^v = r_1^v + 1, \quad r_1^v \geq -1, \quad r_2^v = \max\{r_1^v - 1, -1\}.$$

The finite element spaces for scalar functions $\mathbb{V}_{k+1}^{\text{curl}}(\mathcal{T}_h; \mathbf{r}_0)$ and $\mathbb{V}_{k-1}^{L^2}(\mathcal{T}_h; \mathbf{r}_2)$ remain unchanged. Next we define the finite element space for $\mathbf{H}(\text{div}, \Omega)$ with parameters $\mathbf{r}_1 = (r_1^v, -1)$. The vector function is not continuous on edges. But to be $H(\text{div})$ -conforming, the normal component should be continuous. A refined notation for the smoothness parameter would be: $\mathbf{r}_1 = \begin{pmatrix} r_1^v \\ -1, 0 \end{pmatrix}$ where the tangential component is -1 (discontinuous) and the normal component is 0 (continuous). To simplify notation, we still use the simplified form $\mathbf{r}_1 = (r_1^v, -1)$ and understand that $r_1^e = -1$ means the normal continuity.

Take $\mathbb{P}_k(T; \mathbb{R}^2)$ with $k \geq \max\{2r_1^v + 2, 1\}$ as the space of shape functions. For $r_1^v \geq 0$, the DoFs are

$$(34) \quad \nabla^i \mathbf{v}(\mathbf{v}), \quad \mathbf{v} \in \Delta_0(T), i = 0, \dots, r_1^v,$$

$$(35) \quad \int_e \mathbf{v} \cdot \mathbf{n} q \, ds, \quad \mathbf{q} \in \mathbb{P}_{k-2(r_1^v+1)}(e), e \in \Delta_1(T),$$

$$(36) \quad \int_e \mathbf{v} \cdot \mathbf{t} q \, ds, \quad \mathbf{q} \in \mathbb{P}_{k-2(r_1^v+1)}(e), e \in \Delta_1(T),$$

$$(37) \quad \int_T \mathbf{v} \cdot \mathbf{q} \, dx, \quad \mathbf{q} \in \mathbb{B}_k^2((r_1^v, 0)).$$

Although $r_1^e = -1$, we still use $\mathbb{B}_k((r_1^v, 0))$ as the interior moments so that we can have DoFs (35)-(36) on edges. Namely locally we use vector $(r_1^v, 0)$ Hermite element. When defining the global $H(\text{div})$ -conforming finite element space, the tangential component (36) is considered as local, i.e., double valued on interior edges.

When $r_1^v = -1$, there is no DoFs on vertices and DoFs are

$$(38) \quad \int_e \mathbf{v} \cdot \mathbf{n} q \, ds, \quad \mathbf{q} \in \mathbb{P}_k(e), e \in \Delta_1(T),$$

$$(39) \quad \int_e \mathbf{v} \cdot \mathbf{t} q \, ds, \quad \mathbf{q} \in \mathbb{P}_{k-2}(e), e \in \Delta_1(T),$$

$$(40) \quad \int_T \mathbf{v} \cdot \mathbf{q} \, dx, \quad \mathbf{q} \in \mathbb{B}_k^2((0, 0)).$$

The normal component is the full degree polynomial $\mathbb{P}_k(e)$ but the tangential component is corresponding to the edge bubble $b_e \mathbb{P}_{k-2}(e)$. The interior moments become $\mathbb{B}_k((0, 0))$. Locally we use vector Lagrange finite element but choose different coordinates at different sub-simplices. At each edge, we use $t - n$ (tangential-normal) coordinate and at a vertex we use the coordinate formed by the two normal direction of two edges containing that vertex. Then the uni-solvence in one triangle is trivial and by treating $\mathbf{v} \cdot \mathbf{t}$ as an $H(\text{div})$ bubble function, i.e., (39) is not single-valued, but (38) on $\mathbf{v} \cdot \mathbf{n}$ is, we obtain $H(\text{div})$ -conforming elements. Such $t - n$ decomposition can be generalized to arbitrary dimension and $H(\text{div})$ -conforming tensor finite elements [17].

DoFs (34)-(37) with $r_1^v = 0$ lead to the Stenberg element [31, 19], which is continuous at vertices. If redistribute $\mathbf{v}(\mathbf{v})$ edgewise, we get the Brezzi-Douglas-Marini (BDM)

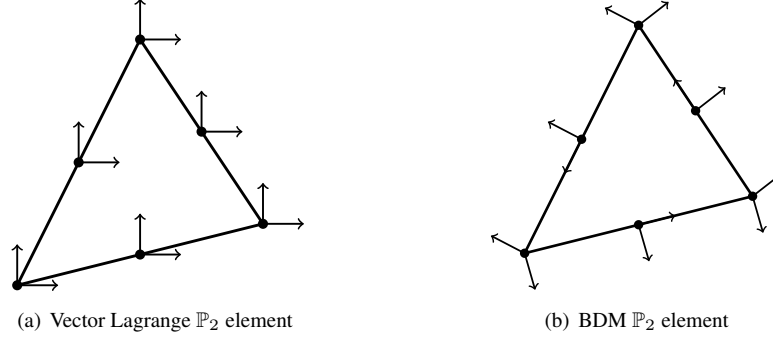


FIGURE 4. Comparison of vector Lagrange element and BDM element.

element [11] with DoFs (38)-(40). In the classical DoFs of BDM, the tangential moment (39) on edges can be further merged into the interior moments; see (51). Here we keep it to emphasize the construction based on the lattice for which the uni-solvence is trivial.

Lemma 4.5. *The DoFs (34)-(37) are uni-solvent for $\mathbb{P}_k(T; \mathbb{R}^2)$ for $k \geq 2r_1^v + 2$ when $r_1^v \geq 0$, and the DoFs (38)-(40) are uni-solvent for $\mathbb{P}_k(T; \mathbb{R}^2)$ for $k \geq 1$ when $r_1^v = -1$.*

Proof. When $r_1^v \geq 0$, it is the vector form of finite element with parameters $(r_1^v, 0)$ and the unisolvence follows from Theorem 3.6.

Now consider $r_1^v = -1$. DoF (38) will determine $\mathbf{v} \cdot \mathbf{n}|_e \in \mathbb{P}_k(e)$. Then at each vertex \mathbf{v} , the two components $\mathbf{v} \cdot \mathbf{n}_1$ and $\mathbf{v} \cdot \mathbf{n}_2$ will determine $\mathbf{v}(\mathbf{v})$. Then the unisolvence follows from the vector form of Lagrange element. \square

Define the global $H(\text{div})$ -conforming finite element space

$$\mathbb{V}_k^{\text{div}}(\mathcal{T}_h; (r_1^v, -1)) = \{\mathbf{v} \in \mathbf{L}^2(\Omega; \mathbb{R}^2) : \mathbf{v}|_T \in \mathbb{P}_k(T; \mathbb{R}^2) \forall T \in \mathcal{T}_h, \\ \text{all the DoFs (34)-(35) are single-valued}\},$$

for $r_1^v \geq 0$, and

$$\mathbb{V}_k^{\text{div}}(\mathcal{T}_h; (-1, -1)) = \{\mathbf{v} \in \mathbf{L}^2(\Omega; \mathbb{R}^2) : \mathbf{v}|_T \in \mathbb{P}_k(T; \mathbb{R}^2) \forall T \in \mathcal{T}_h, \\ \text{DoF (38) is single-valued}\},$$

where the tangential component (36) and (39) are considered as local and thus double-valued for each interior edge.

Theorem 4.6. *Assume parameters $\mathbf{r}_0, \mathbf{r}_1, \mathbf{r}_2$ satisfy*

$$r_0^v = r_1^v + 1, \quad r_1^v \geq -1, \quad r_2^v = \max\{r_1^v, 0\} - 1, \\ r_0^e = 0, \quad r_1^e = -1, \quad r_2^e = -1.$$

Let $k \geq \max\{2r_1^v + 2, 1\}$. The finite element complex

$$(41) \quad \mathbb{R} \xrightarrow{\subset} \mathbb{V}_{k+1}^{\text{curl}}(\mathcal{T}_h; \mathbf{r}_0) \xrightarrow{\text{curl}} \mathbb{V}_k^{\text{div}}(\mathcal{T}_h; \mathbf{r}_1) \xrightarrow{\text{div}} \mathbb{V}_{k-1}^{L^2}(\mathcal{T}_h; \mathbf{r}_2) \rightarrow 0$$

is exact.

Proof. Apparently (41) is a complex, and

$$\text{curl } \mathbb{V}_{k+1}^{\text{curl}}(\mathcal{T}_h; \mathbf{r}_0) = \mathbb{V}_k^{\text{div}}(\mathcal{T}_h; \mathbf{r}_1) \cap \ker(\text{div}).$$

Then we count the dimension. The dimension count in Lemma 4.1 is still valid except $C_{11} = k - 1 - 2r_1^v$. As $C_{01} = k - 2r_0^v$ and $C_{21} = 0$, the identity $C_{01} - C_{11} + C_{21} = -1$ still holds. The rest of the proof is the same as that of Theorem 4.3. \square

Example 4.7. For $k \geq 1$, $r_0^v = 0$, $r_1^v = -1$, $r_2^v = -1$, we recover the standard finite element de Rham complex

$$\mathbb{R} \xrightarrow{\subset} \text{Lagrange}_{k+1}\left(\begin{pmatrix} 0 \\ 0 \end{pmatrix}\right) \xrightarrow{\text{curl}} \text{BDM}_k\left(\begin{pmatrix} -1 \\ -1 \end{pmatrix}\right) \xrightarrow{\text{div}} \text{DG}_{k-1}\left(\begin{pmatrix} -1 \\ -1 \end{pmatrix}\right) \rightarrow 0.$$

We can choose $r_0^v = 1$, $r_1^v = 0$, $r_2^v = -1$ and $k \geq 2$ to get

$$\mathbb{R} \xrightarrow{\subset} \text{Herm}_{k+1}\left(\begin{pmatrix} 1 \\ 0 \end{pmatrix}\right) \xrightarrow{\text{curl}} \text{Sten}_k\left(\begin{pmatrix} 0 \\ -1 \end{pmatrix}\right) \xrightarrow{\text{div}} \text{DG}_{k-1}\left(\begin{pmatrix} -1 \\ -1 \end{pmatrix}\right) \rightarrow 0,$$

which has been constructed in [19].

4.3. General cases with inequality constraint. We consider more general cases with an inequality constraint on the smoothness parameters \mathbf{r}_1 and \mathbf{r}_2 :

$$\mathbf{r}_0 = \mathbf{r}_1 + 1, \quad \mathbf{r}_1 \geq -1, \quad \mathbf{r}_2 \geq \max\{\mathbf{r}_1 - 1, -1\}.$$

To define the finite element spaces, we further require

$$r_1^v \geq 2r_1^e + 1, \quad r_2^v \geq 2r_2^e, \quad k \geq \max\{2r_1^v + 2, 2r_2^v + 2, 1\}, \quad \dim \mathbb{B}_{k-1}(\mathbf{r}_2) \geq 1.$$

The finite element spaces for scalar functions $\mathbb{V}_{k+1}^{\text{curl}}(\mathcal{T}_h; \mathbf{r}_0)$ and $\mathbb{V}_{k-1}^{L^2}(\mathcal{T}_h; \mathbf{r}_2)$ remain unchanged. Next we define a new finite element space for $\mathbf{H}(\text{div}, \Omega)$. Take $\mathbb{P}_k(T; \mathbb{R}^2)$ as the space of shape functions. The degrees of freedom are

$$(42) \quad \nabla^i \mathbf{v}(\mathbf{v}), \quad \mathbf{v} \in \Delta_0(T), i = 0, \dots, r_1^v,$$

$$(43) \quad \nabla^j \text{div} \mathbf{v}(\mathbf{v}), \quad \mathbf{v} \in \Delta_0(T), j = \max\{r_1^v, 0\}, \dots, r_2^v,$$

$$(44) \quad \int_e \mathbf{v} \cdot \mathbf{n} q \, ds, \quad q \in \mathbb{P}_{k-2(r_1^v+1)}(e), e \in \Delta_1(T),$$

$$(45) \quad \int_e \partial_n^i (\mathbf{v} \cdot \mathbf{t}) q \, ds, \quad q \in \mathbb{P}_{k-2(r_1^v+1)+i}(e), e \in \Delta_1(T), i = 0, \dots, r_1^e,$$

$$(46) \quad \int_e \partial_n^i (\text{div} \mathbf{v}) q \, ds, \quad q \in \mathbb{P}_{k-1-2(r_2^v+1)+i}(e), e \in \Delta_1(T), i = 0, \dots, r_2^e,$$

$$(47) \quad \int_T \text{div} \mathbf{v} q \, dx, \quad q \in \mathbb{B}_{k-1}(\mathbf{r}_2)/\mathbb{R},$$

$$(48) \quad \int_T \mathbf{v} \cdot \mathbf{q} \, dx, \quad \mathbf{q} \in \text{curl} \mathbb{B}_{k+1}(\mathbf{r}_1 + 1).$$

Lemma 4.8. *The DoFs (42)-(48) are uni-solvent for $\mathbb{P}_k(T; \mathbb{R}^2)$.*

Proof. The number of DoFs (43) and (46)-(47) is $\dim \mathbb{P}_{k-1}(T) - 3\binom{r_1^v+1}{2} - 1$, which is constant with respect to \mathbf{r}_2 . Hence the number of DoFs (42)-(48) is also constant with respect to \mathbf{r}_2 . As a result the number of DoFs (42)-(48) equals to $\dim \mathbb{P}_k(T; \mathbb{R}^2)$, which has been proved for case $\mathbf{r}_2 = \max\{\mathbf{r}_1 - 1, -1\}$.

Take $\mathbf{v} \in \mathbb{P}_k(T; \mathbb{R}^2)$ and assume all the DoFs (42)-(48) vanish. The vanishing DoF (44) implies $\text{div} \mathbf{v} \in L_0^2(T)$. By the vanishing DoFs (42)-(43) and (46)-(47), we get $\text{div} \mathbf{v} = 0$. And it follows from the vanishing DoFs (42) and (44)-(45) that $\mathbf{v} \in \text{curl} \mathbb{B}_{k+1}(\mathbf{r}_1 + 1)$. Therefore $\mathbf{v} = \mathbf{0}$ holds from the vanishing DoF (48). \square

Define global $C^{r_1^e}$ -continuous finite element space

$$\mathbb{V}_k^{\text{div}}(\mathcal{T}_h; \mathbf{r}_1, \mathbf{r}_2) = \{\mathbf{v} \in \mathbf{L}^2(\Omega; \mathbb{R}^2) : \mathbf{v}|_T \in \mathbb{P}_k(T; \mathbb{R}^2) \forall T \in \mathcal{T}_h, \\ \text{all the DoFs (42)-(46) are single-valued}\}.$$

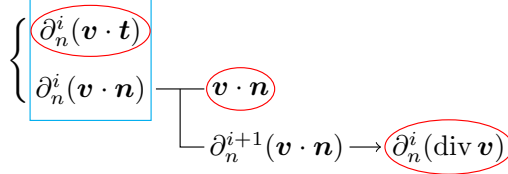


FIGURE 5. Change of DoFs: DoF (28) is in the blue rectangle and (44), (45), and (46) are in the red circle. They are equivalent when $r_2^e = r_1^e - 1 \geq 0$.

For $i = 0, 1, \dots, r_1^e - 1$ with $r_2^e = r_1^e - 1 \geq 0$,

$$\partial_n^i(\text{div } \mathbf{v}) = \partial_n^i(\partial_n(\mathbf{v} \cdot \mathbf{n}) + \partial_t(\mathbf{v} \cdot \mathbf{t})) = \partial_n^{i+1}(\mathbf{v} \cdot \mathbf{n}) + \partial_t(\partial_n^i(\mathbf{v} \cdot \mathbf{t})).$$

The second part $\partial_t(\partial_n^i(\mathbf{v} \cdot \mathbf{t}))$ will be determined by (42) and (45). That is a linear combination of (44), (45), and (46) will determine (28). Consequently it returns to the finite element defined before. When $r_2 \geq r_1 - 1$, we have

$$\mathbb{V}_k^{\text{div}}(\mathcal{T}_h; \mathbf{r}_1, \mathbf{r}_2) \subseteq \mathbb{V}_k^{\text{div}}(\mathcal{T}_h; \mathbf{r}_1, \mathbf{r}_1 - 1).$$

Namely additional smoothness on $\text{div } \mathbf{v}$ is imposed. The change of DoFs is illustrated in Fig. 5.

Theorem 4.9. *Let $\mathbf{r}_0 = \mathbf{r}_1 + 1, \mathbf{r}_1 \geq -1, \mathbf{r}_2 \geq \max\{\mathbf{r}_1 - 1, -1\}$ satisfying $r_1^v \geq 2r_1^e + 1, r_2^v \geq 2r_2^e$. Assume $k \geq \max\{2r_1^v + 2, 2r_2^v + 2, 1\}$ and $\dim \mathbb{B}_{k-1}(\mathbf{r}_2) \geq 1$. The finite element complex*

$$(49) \quad \mathbb{R} \xrightarrow{\subset} \mathbb{V}_{k+1}^{\text{curl}}(\mathcal{T}_h; \mathbf{r}_0) \xrightarrow{\text{curl}} \mathbb{V}_k^{\text{div}}(\mathcal{T}_h; \mathbf{r}_1, \mathbf{r}_2) \xrightarrow{\text{div}} \mathbb{V}_{k-1}^{L^2}(\mathcal{T}_h; \mathbf{r}_2) \rightarrow 0$$

is exact.

Proof. It is straightforward to verify that (49) is a complex by showing $\text{curl } \mathbb{V}_{k+1}^{\text{curl}}(\mathcal{T}_h; \mathbf{r}_0) \subseteq \mathbb{V}_k^{\text{div}}(\mathcal{T}_h; \mathbf{r}_1, \mathbf{r}_2)$ and $\text{div } \mathbb{V}_k^{\text{div}}(\mathcal{T}_h; \mathbf{r}_1, \mathbf{r}_2) \subseteq \mathbb{V}_{k-1}^{L^2}(\mathcal{T}_h; \mathbf{r}_2)$. It is also obvious that

$$\text{curl } \mathbb{V}_{k+1}^{\text{curl}}(\mathcal{T}_h; \mathbf{r}_0) = \mathbb{V}_k^{\text{div}}(\mathcal{T}_h; \mathbf{r}_1, \mathbf{r}_2) \cap \ker(\text{div}).$$

We have proved the exactness for $\mathbf{r}_2 = \max\{\mathbf{r}_1 - 1, -1\}$. When counting the dimension, only check the difference.

The added vertices DoFs for $\mathbb{V}_k^{\text{div}}(\mathcal{T}_h; \mathbf{r}_1, \mathbf{r}_2)$ and $\mathbb{V}_{k-1}^{L^2}(\mathcal{T}_h; \mathbf{r}_2)$ are equal, i.e.,

$$C_{10}(\mathbf{r}_2) - C_{10}(\max\{\mathbf{r}_1 - 1, -1\}) = C_{20}(\mathbf{r}_2) - C_{20}(\max\{\mathbf{r}_1 - 1, -1\}).$$

Same argument can be applied to edge DoFs. Therefore the alternating column sums remains the same and the proof of Theorem 4.3 can be still applied. \square

We use Figure 6 to illustrate the exactness of the finite element de Rham complex (49), which is obtained by adding more constraints on $\text{div } \mathbf{v}$.

Let $\mathbb{B}_k^{\text{div}}(\mathbf{r}_1, \mathbf{r}_2) := \{\mathbf{v} \in \mathbb{P}_k(T; \mathbb{R}^2) : \text{all the DoFs (42)-(46) vanish}\}$, then

$$(50) \quad \dim \mathbb{B}_k^{\text{div}}(\mathbf{r}_1, \mathbf{r}_2) = \dim \mathbb{B}_{k-1}(\mathbf{r}_2) + \dim \mathbb{B}_{k+1}(\mathbf{r}_1 + 1) - 1.$$

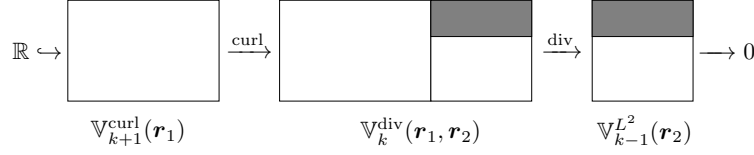


FIGURE 6. Explanation of the smooth finite element de Rham complex with increased smoothness in pressure. Spaces are corresponding to white boxes and the darker gray part denotes the extra constraints on $\operatorname{div} \mathbf{v}$.

DoFs (47)-(48) can be combined as

$$(51) \quad \int_T \mathbf{v} \cdot \mathbf{q} \, dx, \quad \mathbf{q} \in \mathbb{B}_k^{\operatorname{div}}(\mathbf{r}_1, \mathbf{r}_2).$$

When $\mathbf{r}_1 \geq 0$ and $\mathbf{r}_2 = \mathbf{r}_1 - 1$, we have $\mathbb{B}_k^{\operatorname{div}}(\mathbf{r}_1, \mathbf{r}_2) = \mathbb{B}_k^2(\mathbf{r}_1)$. When $r_1^e = -1$, the shape function dual to the tangential DoFs (36) or (39) are also included in $\mathbb{B}_k^{\operatorname{div}}(\mathbf{r}_1, \mathbf{r}_2)$.

Corollary 4.10. *Let $\mathbf{r}_0 = \mathbf{r}_1 + 1$, $\mathbf{r}_1 \geq -1$, $\mathbf{r}_2 \geq \max\{\mathbf{r}_1 - 1, -1\}$ satisfying $r_1^v \geq 2r_1^e + 1$, $r_2^v \geq 2r_2^e$. Let $k \geq \max\{2r_1^v + 2, 2r_2^v + 2, 1\}$ and $\dim \mathbb{B}_{k-1}(\mathbf{r}_2) \geq 1$. The following bubble complex*

$$(52) \quad 0 \xrightarrow{\subset} \mathbb{B}_{k+1}(\mathbf{r}_0) \xrightarrow{\operatorname{curl}} \mathbb{B}_k^{\operatorname{div}}(\mathbf{r}_1, \mathbf{r}_2) \xrightarrow{\operatorname{div}} \mathbb{B}_{k-1}(\mathbf{r}_2) \xrightarrow{Q_0} \mathbb{R} \rightarrow 0$$

is exact.

Proof. Apparently (52) is a complex, and $\operatorname{curl} \mathbb{B}_{k+1}(\mathbf{r}_0) = \mathbb{B}_k^{\operatorname{div}}(\mathbf{r}_1, \mathbf{r}_2) \cap \ker(\operatorname{div})$. The exactness then follows from the dimension count (50). \square

We present two examples of the de Rham complex ending with the Lagrange element.

Example 4.11. Consider the case $\mathbf{r}_1 = (1, 0)$, $\mathbf{r}_2 = 0$ and $k \geq 4$, which is also constructed as $H^1(\operatorname{div}) - H^1$ Stokes pair in Falk and Neilan [23]. Now we can choose continuous pressure space without increasing the polynomial degree. The complex is

$$\mathbb{R} \xrightarrow{\subset} \operatorname{Argy}_{k+1} \left(\begin{pmatrix} 2 \\ 1 \end{pmatrix} \right) \xrightarrow{\operatorname{curl}} \mathbb{V}_k^{\operatorname{div}} \left(\begin{pmatrix} 1 \\ 0 \end{pmatrix}, \begin{pmatrix} 0 \\ 0 \end{pmatrix} \right) \xrightarrow{\operatorname{div}} \operatorname{Lagrange}_{k-1} \left(\begin{pmatrix} 0 \\ 0 \end{pmatrix} \right) \rightarrow 0.$$

The velocity space is a reduced Hermite space with continuity of $\operatorname{div} \mathbf{v}$ at vertices and edges. With such modification, this $\mathbb{P}_k - \mathbb{P}_{k-1}$ Stokes pair with continuous pressure element is point-wise divergence free comparing to the Taylor-Hood element.

Example 4.12. Consider the case $\mathbf{r}_1 = -1$ and $\mathbf{r}_2 = 0$, and $k \geq 4$. The complex is

$$\mathbb{R} \xrightarrow{\subset} \operatorname{Lagrange}_{k+1} \left(\begin{pmatrix} 0 \\ 0 \end{pmatrix} \right) \xrightarrow{\operatorname{curl}} \mathbb{V}_k^{\operatorname{div}} \left(\begin{pmatrix} -1 \\ -1 \end{pmatrix}, \begin{pmatrix} 0 \\ 0 \end{pmatrix} \right) \xrightarrow{\operatorname{div}} \operatorname{Lagrange}_{k-1} \left(\begin{pmatrix} 0 \\ 0 \end{pmatrix} \right) \rightarrow 0,$$

which is the rotation of the finite element de Rham complex in [27, Section 5.2.1]. The space $\mathbb{V}_k^{\operatorname{div}}(\mathcal{T}_h; \mathbf{r}_1, \mathbf{r}_0)$ can be used to discretize fourth-order div or curl equations [24, 27]. We can also apply the pair $\mathbb{V}_k^{\operatorname{div}}(\mathcal{T}_h; \mathbf{r}_1, \mathbf{r}_0)$ and $\operatorname{Lagrange}_{k-1}(\mathcal{T}_h; \mathbf{r}_0)$ to mixed finite element methods for Poisson equation $-\Delta u = f$, in which the discrete u_h is continuous.

For simplicity, hereafter we will omit the triangulation \mathcal{T}_h in the notation of global finite element spaces. For example, $\mathbb{V}_k^{\operatorname{div}}(\mathcal{T}_h; \mathbf{r}_1, \mathbf{r}_2)$ will be abbreviated as $\mathbb{V}_k^{\operatorname{div}}(\mathbf{r}_1, \mathbf{r}_2)$.

5. BEYOND DE RHAM COMPLEXES

In this section, we shall mainly use BGG approach [7] to construct more finite element complexes from copies of finite element de Rham complexes. In two dimensions, the induced complexes are elasticity and divdiv complexes, and by rotation, Hessian and rot-rot complexes.

5.1. Finite element curl div complexes. Based on the finite element de Rham complex (49), we can obtain the finite element discretization of the curl div complex [7]

$$\mathbb{R} \times \{0\} \xrightarrow{\subset} H^1(\Omega) \times \mathbb{R} \xrightarrow{(\text{curl}, \boldsymbol{x})} \mathbf{H}(\text{curl div}, \Omega) \xrightarrow{\text{curl div}} \mathbf{H}(\text{div}, \Omega) \xrightarrow{\text{div}} L^2(\Omega) \rightarrow 0,$$

where $\mathbf{H}(\text{curl div}, \Omega) := \mathbf{H}^{0,1}(\text{div}, \Omega) = \{\mathbf{v} \in \mathbf{H}(\text{div}, \Omega) : \text{div } \mathbf{v} \in H^1(\Omega)\}$.

Theorem 5.1. *Let $\mathbf{r}_0 = \mathbf{r}_1 + 1$, $\mathbf{r}_1 \geq -1$, $\mathbf{r}_2 \geq \max\{\mathbf{r}_1 - 1, 0\}$, $\mathbf{r}_3 \geq \max\{\mathbf{r}_2 - 2, -1\}$ satisfying $r_1^y \geq 2r_1^e + 1$, $r_2^y \geq 2r_2^e$, $r_3^y \geq 2r_3^e$. Assume $k \geq \max\{2r_1^y + 2, 2r_2^y + 2, 2r_3^y + 4, 3\}$ and $\dim \mathbb{B}_{k-1}(\mathbf{r}_2) \geq 1$, $\dim \mathbb{B}_{k-3}(\mathbf{r}_3) \geq 1$. The finite element complex*

$$(53) \quad \mathbb{R} \times \{0\} \xrightarrow{\subset} \mathbb{V}_{k+1}^{\text{curl}}(\mathbf{r}_0) \times \mathbb{R} \xrightarrow{(\text{curl}, \boldsymbol{x})} \mathbb{V}_k^{\text{div}}(\mathbf{r}_1, \mathbf{r}_2) \xrightarrow{\text{curl div}} \mathbb{V}_{k-2}^{\text{div}}(\mathbf{r}_2 - 1, \mathbf{r}_3) \xrightarrow{\text{div}} \mathbb{V}_{k-3}^{L^2}(\mathbf{r}_3) \rightarrow 0$$

is exact.

Proof. By complex (49), clearly (53) is a complex, and $\text{div } \mathbb{V}_{k-2}^{\text{div}}(\mathbf{r}_2 - 1, \mathbf{r}_3) = \mathbb{V}_{k-3}^{L^2}(\mathbf{r}_3)$. We will focus on the exactness of complex (53).

We get from the exactness of complex (49) that

$$\text{div } \mathbb{V}_k^{\text{div}}(\mathbf{r}_1, \mathbf{r}_2) = \mathbb{V}_{k-1}^{L^2}(\mathbf{r}_2), \quad \text{curl } \mathbb{V}_{k-1}^{\text{curl}}(\mathbf{r}_2) = \mathbb{V}_{k-2}^{\text{div}}(\mathbf{r}_2 - 1, \mathbf{r}_3) \cap \ker(\text{div}).$$

Hence $\text{curl div } \mathbb{V}_k^{\text{div}}(\mathbf{r}_1, \mathbf{r}_2) = \mathbb{V}_{k-2}^{\text{div}}(\mathbf{r}_2 - 1, \mathbf{r}_3) \cap \ker(\text{div})$ follows from $\mathbb{V}_{k-1}^{\text{curl}}(\mathbf{r}_2) = \mathbb{V}_{k-1}^{L^2}(\mathbf{r}_2)$ when $\mathbf{r}_2 \geq 0$.

For $\mathbf{v} \in \mathbb{V}_k^{\text{div}}(\mathbf{r}_1, \mathbf{r}_2) \cap \ker(\text{curl div})$, there exists constant c such that $\text{div } \mathbf{v} = 2c$. Then we have $\text{div}(\mathbf{v} - c\boldsymbol{x}) = 0$, i.e., $\mathbf{v} - c\boldsymbol{x} \in \mathbb{V}_k^{\text{div}}(\mathbf{r}_1, \mathbf{r}_2) \cap \ker(\text{div})$. Therefore $\mathbf{v} \in \text{curl } \mathbb{V}_{k+1}^{\text{curl}}(\mathbf{r}_0) \oplus \boldsymbol{x}\mathbb{R}$ holds from the exactness of complex (49). \square

5.2. Finite element elasticity and Hessian complexes. We first present two examples. Denote by

$$\mathbb{V}_k^{\text{div}}(\mathbf{r}_1, \mathbf{r}_2; \mathbb{M}) := \mathbb{V}_k^{\text{div}}(\mathbf{r}_1, \mathbf{r}_2) \times \mathbb{V}_k^{\text{div}}(\mathbf{r}_1, \mathbf{r}_2).$$

To fit the space, we skip the constant space \mathbb{R} in the beginning and 0 at the end in the sequence, and \mathcal{T}_h in the spaces. The first one has been presented in [19]:

$$\begin{array}{ccccc} \text{Argy}_{k+2}\left(\begin{pmatrix} 2 \\ 1 \end{pmatrix}\right) & \xrightarrow{\text{curl}} & \text{Herm}_{k+1}\left(\begin{pmatrix} 1 \\ 0 \end{pmatrix}; \mathbb{R}^2\right) & \xrightarrow{\text{div}} & \mathbb{V}_k^{L^2}\left(\begin{pmatrix} 0 \\ -1 \end{pmatrix}\right) \\ & \nearrow \text{id} & & \nearrow -2 \text{sskw} & \\ \text{Herm}_{k+1}\left(\begin{pmatrix} 1 \\ 0 \end{pmatrix}; \mathbb{R}^2\right) & \xrightarrow{\text{curl}} & \text{Sten}_k\left(\begin{pmatrix} 0 \\ -1 \end{pmatrix}; \mathbb{M}\right) & \xrightarrow{\text{div}} & \text{DG}_{k-1}\left(\begin{pmatrix} -1 \\ -1 \end{pmatrix}; \mathbb{R}^2\right) \end{array}$$

This will lead to the elasticity complex and with rotation to the Hessian complex:

$$\mathbf{RM} \xrightarrow{\subset} \text{Argy}_{k+2}\left(\begin{pmatrix} 2 \\ 1 \end{pmatrix}\right) \xrightarrow{\text{Air}} \text{HZ}_k\left(\begin{pmatrix} 0 \\ -1 \end{pmatrix}; \mathbb{S}\right) \xrightarrow{\text{div}} \text{DG}_{k-1}\left(\begin{pmatrix} -1 \\ -1 \end{pmatrix}; \mathbb{R}^2\right) \rightarrow \mathbf{0}.$$

The finite element elasticity complex based on Arnold-Winther element [8] was reconstructed in [4] by a different discrete BGG diagram.

We then present another example with rotated differential operators and use $\mathbb{V}^{\text{rot}}(\mathbf{r}_1, \mathbf{r}_2)$ to increase the smoothness of the last space. The finite element BGG diagram

$$\begin{array}{ccccc} \text{Argy}_{k+2}\left(\begin{pmatrix} 2 \\ 1 \end{pmatrix}\right) & \xrightarrow{\text{grad}} & \text{Herm}_{k+1}\left(\begin{pmatrix} 1 \\ 0 \end{pmatrix}; \mathbb{R}^2\right) & \xrightarrow{\text{rot}} & \mathbb{V}_k^{L^2}\left(\begin{pmatrix} 0 \\ -1 \end{pmatrix}\right) \\ & \nearrow \text{id} & & \nearrow -2 \text{sskw} & \\ \text{Herm}_{k+1}\left(\begin{pmatrix} 1 \\ 0 \end{pmatrix}; \mathbb{R}^2\right) & \xrightarrow{\text{grad}} & \mathbb{V}_k^{\text{rot}}\left(\begin{pmatrix} 0 \\ -1 \end{pmatrix}, \begin{pmatrix} 0 \\ 0 \end{pmatrix}; \mathbb{M}\right) & \xrightarrow{\text{rot}} & \text{Lagrange}_{k-1}\left(\begin{pmatrix} 0 \\ 0 \end{pmatrix}; \mathbb{R}^2\right) \end{array}$$

will lead to the finite element Hessian complex constructed in [15]

$$\mathbb{P}_1 \xrightarrow{\subset} V_h^{\text{hess}} \xrightarrow{\nabla^2} \Sigma_h^{\text{rot}} \xrightarrow{\text{rot}} \mathbf{V}_h^{\text{grad}} \rightarrow \mathbf{0}.$$

We now present the general case.

Theorem 5.2. *Let $\mathbf{r}_1 \geq -1$ and $\mathbf{r}_2 \geq \max\{\mathbf{r}_1 - 1, -1\}$ satisfying $r_1^v \geq 2r_1^e + 2$, $r_2^v \geq 2r_2^e$, and let polynomial degree $k \geq \max\{2r_1^v + 3, 2r_2^v + 2\}$ such that $\dim \mathbb{B}_{k-1}^2(\mathbf{r}_2) \geq 3$. Then we have the BGG diagram*

$$(54) \quad \begin{array}{ccccccc} \mathbb{R} & \xrightarrow{\subset} & \mathbb{V}_{k+2}^{\text{curl}}(\mathbf{r}_1 + 2) & \xrightarrow{\text{curl}} & \mathbb{V}_{k+1}^{\text{div}}(\mathbf{r}_1 + 1) & \xrightarrow{\text{div}} & \mathbb{V}_k^{L^2}(\mathbf{r}_1) \longrightarrow 0 \\ & & \nearrow \text{id} & & \nearrow -2 \text{sskw} & & \\ \mathbb{R} & \xrightarrow{\subset} & \mathbb{V}_{k+1}^{\text{curl}}(\mathbf{r}_1 + 1; \mathbb{R}^2) & \xrightarrow{\text{curl}} & \mathbb{V}_k^{\text{div}}(\mathbf{r}_1, \mathbf{r}_2; \mathbb{M}) & \xrightarrow{\text{div}} & \mathbb{V}_{k-1}^{L^2}(\mathbf{r}_2; \mathbb{R}^2) \longrightarrow 0 \end{array}$$

which leads to the finite element elasticity complex

$$(55) \quad \mathbb{P}_1 \xrightarrow{\subset} \mathbb{V}_{k+2}^{\text{curl}}(\mathbf{r}_1 + 2) \xrightarrow{\text{Air}} \mathbb{V}_k^{\text{div}}(\mathbf{r}_1, \mathbf{r}_2; \mathbb{S}) \xrightarrow{\text{div}} \mathbb{V}_{k-1}^{L^2}(\mathbf{r}_2; \mathbb{R}^2) \rightarrow \mathbf{0},$$

where $\mathbb{V}_k^{\text{div}}(\mathbf{r}_1, \mathbf{r}_2; \mathbb{S}) := \mathbb{V}_k^{\text{div}}(\mathbf{r}_1, \mathbf{r}_2; \mathbb{M}) \cap \ker(\text{sskw})$.

Proof. First we show that $\text{sskw } \mathbb{V}_k^{\text{div}}(\mathbf{r}_1, \mathbf{r}_2; \mathbb{M}) = \mathbb{V}_k^{L^2}(\mathbf{r}_1)$. For $q \in \mathbb{V}_k^{L^2}(\mathbf{r}_1)$, by the exactness of the complex in the top line of (54), there exists $\mathbf{v}_h \in \mathbb{V}_{k+1}^{\text{div}}(\mathbf{r}_1) = \mathbb{V}_{k+1}^{\text{curl}}(\mathbf{r}_1)$ such that $\text{div } \mathbf{v}_h = q_h$. Then we get from the anti-commutative property (3) that $q_h = 2 \text{sskw}(\text{curl } \mathbf{v}_h)$.

We can apply the BGG framework in [7] to get the complex (55) and its exactness. In two dimensions, we will provide a simple proof without invoking the machinery.

Clearly (55) is a complex. We prove the exactness of complex (55) in two steps.

Step 1. Prove $\text{Air } \mathbb{V}_{k+2}^{\text{curl}}(\mathbf{r}_1 + 2) = \mathbb{V}_k^{\text{div}}(\mathbf{r}_1, \mathbf{r}_2; \mathbb{S}) \cap \ker(\text{div})$. For $\boldsymbol{\tau} \in \mathbb{V}_k^{\text{div}}(\mathbf{r}_1, \mathbf{r}_2; \mathbb{S}) \cap \ker(\text{div})$, by the bottom complex in (54), there exists $\mathbf{v} \in \mathbb{V}_{k+1}^{\text{curl}}(\mathbf{r}_1 + 1; \mathbb{R}^2)$ such that $\boldsymbol{\tau} = \text{curl } \mathbf{v}$. Then it follows from (3) that

$$\text{div } \mathbf{v} = 2 \text{sskw}(\text{curl } \mathbf{v}) = 2 \text{sskw } \boldsymbol{\tau} = 0.$$

By the exactness of the top de Rham complex, there exists $q \in \mathbb{V}_{k+2}^{\text{curl}}(\mathbf{r}_1 + 2)$ such that $\mathbf{v} = \text{curl } q$. Thus $\boldsymbol{\tau} = \text{curl } \mathbf{v} = \text{Air } q \in \text{Air } \mathbb{V}_{k+2}^{\text{curl}}(\mathbf{r}_1 + 2)$.

Step 2. Prove $\text{div } \mathbb{V}_k^{\text{div}}(\mathbf{r}_1, \mathbf{r}_2; \mathbb{S}) = \mathbb{V}_{k-1}^{L^2}(\mathbf{r}_2; \mathbb{R}^2)$. As $\text{div} : \mathbb{V}_k^{\text{div}}(\mathbf{r}_1, \mathbf{r}_2; \mathbb{M}) \rightarrow \mathbb{V}_{k-1}^{L^2}(\mathbf{r}_2; \mathbb{R}^2)$ is surjective, given a $\mathbf{q} \in \mathbb{V}_{k-1}^{L^2}(\mathbf{r}_2; \mathbb{R}^2)$, we can find $\boldsymbol{\tau} \in \mathbb{V}_k^{\text{div}}(\mathbf{r}_1, \mathbf{r}_2; \mathbb{M})$ such that $\text{div } \boldsymbol{\tau} = \mathbf{q}$. By the diagram (54), we can find $\mathbf{v} \in \mathbb{V}_{k+1}^{\text{div}}(\mathbf{r}_1 + 1)$ such that $\text{div } \mathbf{v} = -2 \text{sskw } \boldsymbol{\tau}$. Set $\boldsymbol{\tau}^s = \boldsymbol{\tau} + \text{curl } \mathbf{v}$. Then $\text{div } \boldsymbol{\tau}^s = \text{div } \boldsymbol{\tau} = \mathbf{q}$ and $2 \text{sskw } \boldsymbol{\tau}^s = 2 \text{sskw } \boldsymbol{\tau} + 2 \text{sskw } \text{curl } \mathbf{v} = 2 \text{sskw } \boldsymbol{\tau} + \text{div } \mathbf{v} = 0$, i.e. $\boldsymbol{\tau}^s$ is symmetric. Therefore we find $\boldsymbol{\tau}^s \in \mathbb{V}_k^{\text{div}}(\mathbf{r}_1, \mathbf{r}_2; \mathbb{S})$ and $\text{div } \boldsymbol{\tau}^s = \mathbf{q}$. \square

In (55), $\mathbb{V}_k^{\text{div}}(\mathbf{r}_1, \mathbf{r}_2; \mathbb{S})$ is defined as $\mathbb{V}_k^{\text{div}}(\mathbf{r}_1, \mathbf{r}_2; \mathbb{M}) \cap \ker(\text{sskw})$. Next we give the finite element description of space $\mathbb{V}_k^{\text{div}}(\mathbf{r}_1, \mathbf{r}_2; \mathbb{S})$ and thus can obtain locally supported basis. On each triangle, we take $\mathbb{P}_k(T; \mathbb{S})$ as the shape function space. By symmetrizing DoFs (42)-(48), we propose the following local DoFs for space $\mathbb{V}_k^{\text{div}}(\mathbf{r}_1, \mathbf{r}_2; \mathbb{S})$

$$(56) \quad \nabla^i \boldsymbol{\tau}(\mathbf{v}), \quad \mathbf{v} \in \Delta_0(T), i = 0, \dots, r_1^{\vee},$$

$$(57) \quad \nabla^j \text{div } \boldsymbol{\tau}(\mathbf{v}), \quad \mathbf{v} \in \Delta_0(T), j = r_1^{\vee}, \dots, r_2^{\vee},$$

$$(58) \quad \int_e (\boldsymbol{\tau} \mathbf{n}) \cdot \mathbf{q} \, ds, \quad \mathbf{q} \in \mathbb{P}_{k-2(r_1^{\vee}+1)}^2(e), e \in \Delta_1(T),$$

$$(59) \quad \int_e \partial_n^i (\mathbf{t}^{\top} \boldsymbol{\tau} \mathbf{t}) \, q \, ds, \quad q \in \mathbb{P}_{k-2(r_1^{\vee}+1)+i}(e), e \in \Delta_1(T), i = 0, \dots, r_1^e,$$

$$(60) \quad \int_e \partial_n^i (\text{div } \boldsymbol{\tau}) \cdot \mathbf{q} \, ds, \quad \mathbf{q} \in \mathbb{P}_{k-1-2(r_2^{\vee}+1)+i}^2(e), e \in \Delta_1(T), i = 0, \dots, r_2^e,$$

$$(61) \quad \int_T \text{div } \boldsymbol{\tau} \cdot \mathbf{q} \, dx, \quad \mathbf{q} \in \mathbb{B}_{k-1}^2(\mathbf{r}_2) / \mathbf{RM},$$

$$(62) \quad \int_T \boldsymbol{\tau} \cdot \mathbf{q} \, dx, \quad \mathbf{q} \in \text{Air } \mathbb{B}_{k+2}(\mathbf{r}_1 + 2).$$

Lemma 5.3. *The DoFs (56)-(62) are uni-solvent for $\mathbb{P}_k(T; \mathbb{S})$.*

Proof. The number of DoFs (57) and (60)-(61) is $2 \dim \mathbb{P}_{k-1}(T) - 3 - 6 \binom{r_1^{\vee}+1}{2}$. Then the number of DoFs (56)-(62) is

$$\begin{aligned} & 9 \binom{r_1^{\vee}+2}{2} + 6(k-1-2r_1^{\vee}) + 3 \sum_{i=0}^{r_1^e} (k-1-2r_1^{\vee}+i) + \dim \mathbb{B}_{k+2}(\mathbf{r}_1 + 2) \\ & + 2 \dim \mathbb{P}_{k-1}(T) - 3 - 6 \binom{r_1^{\vee}+1}{2} = \dim \mathbb{P}_{k+2}(T) + 2 \dim \mathbb{P}_{k-1}(T) - 3, \end{aligned}$$

by (9), which equals to $\dim \mathbb{P}_k(T; \mathbb{S})$.

Take $\boldsymbol{\tau} \in \mathbb{P}_k(T; \mathbb{S})$, and assume all the DoFs (56)-(62) vanish. It follows from the integration by parts and (58) that

$$(\text{div } \boldsymbol{\tau}, \mathbf{q})_T = 0 \quad \forall \mathbf{q} \in \mathbf{RM}.$$

Thanks to DoFs (56)-(57) and (60)-(61), we get $\text{div } \boldsymbol{\tau} = \mathbf{0}$. On each edge e ,

$$\begin{aligned} \partial_n^i (\text{div } \boldsymbol{\tau}) &= \partial_n^i (\text{div}(\mathbf{n}^{\top} \boldsymbol{\tau})) \mathbf{n} + \partial_n^i (\text{div}(\mathbf{t}^{\top} \boldsymbol{\tau})) \mathbf{t} \\ &= \partial_n^i (\partial_n(\mathbf{n}^{\top} \boldsymbol{\tau} \mathbf{n}) + \partial_t(\mathbf{n}^{\top} \boldsymbol{\tau} \mathbf{t})) \mathbf{n} + \partial_n^i (\partial_n(\mathbf{t}^{\top} \boldsymbol{\tau} \mathbf{n}) + \partial_t(\mathbf{t}^{\top} \boldsymbol{\tau} \mathbf{t})) \mathbf{t} \\ &= (\partial_n^{i+1}(\mathbf{n}^{\top} \boldsymbol{\tau} \mathbf{n}) + \partial_t \partial_n^i(\mathbf{n}^{\top} \boldsymbol{\tau} \mathbf{t})) \mathbf{n} + (\partial_n^{i+1}(\mathbf{t}^{\top} \boldsymbol{\tau} \mathbf{n}) + \partial_t \partial_n^i(\mathbf{t}^{\top} \boldsymbol{\tau} \mathbf{t})) \mathbf{t} \end{aligned}$$

Then we acquire from DoFs (56)-(60) that $\boldsymbol{\tau} \in \text{Air } \mathbb{B}_{k+2}(\mathbf{r}_1 + 2)$. Finally we get $\boldsymbol{\tau} = \mathbf{0}$ from the vanishing DoF (62). \square

Next we define the global finite element space and show it is $\mathbb{V}_k^{\text{div}}(\mathbf{r}_1, \mathbf{r}_2; \mathbb{S})$.

Lemma 5.4. *It holds*

$$\begin{aligned} \mathbb{V}_k^{\text{div}}(\mathbf{r}_1, \mathbf{r}_2; \mathbb{S}) &= \mathbb{V} := \{ \boldsymbol{\tau} \in \mathbf{L}^2(\Omega; \mathbb{S}) : \boldsymbol{\tau}|_T \in \mathbb{P}_k(T; \mathbb{S}) \forall T \in \mathcal{T}_h, \\ &\quad \text{all the DoFs (56)-(60) are single-valued} \}. \end{aligned}$$

Proof. Apparently $\mathbb{V} \subseteq \mathbb{V}_k^{\text{div}}(\mathbf{r}_1, \mathbf{r}_2; \mathbb{S})$. It suffices to show $\dim \mathbb{V}_k^{\text{div}}(\mathbf{r}_1, \mathbf{r}_2; \mathbb{S}) = \dim \mathbb{V}$. By comparing DoFs and direct computation,

$$\begin{aligned}
& \dim \mathbb{V} - \dim \mathbb{V}_{k-1}^{L^2}(\mathbf{r}_2; \mathbb{R}^2) \\
&= 3 \binom{r_1^v + 2}{2} |\Delta_0(\mathcal{T}_h)| - 2 \binom{r_1^v + 1}{2} |\Delta_0(\mathcal{T}_h)| + 2(k-1 - 2r_1^v) |\Delta_1(\mathcal{T}_h)| \\
&\quad + |\Delta_1(\mathcal{T}_h)| \sum_{i=0}^{r_1^e} (k-1 - 2r_1^v + i) + |\Delta_2(\mathcal{T}_h)| (\dim \mathbb{B}_{k+2}(\mathbf{r}_1 + 2) - 3) \\
&= |\Delta_0(\mathcal{T}_h)| \binom{r_1^v + 4}{2} + |\Delta_1(\mathcal{T}_h)| \sum_{i=0}^{r_1^e + 2} (k-3 - 2r_1^v + i) \\
&\quad + |\Delta_2(\mathcal{T}_h)| \dim \mathbb{B}_{k+2}(\mathbf{r}_1 + 2) - 3(|\Delta_0(\mathcal{T}_h)| - |\Delta_1(\mathcal{T}_h)| + |\Delta_2(\mathcal{T}_h)|) \\
&= \dim \mathbb{V}_{k+2}^{\text{curl}}(\mathbf{r}_1 + 2) - 3(|\Delta_0(\mathcal{T}_h)| - |\Delta_1(\mathcal{T}_h)| + |\Delta_2(\mathcal{T}_h)|),
\end{aligned}$$

which together with the Euler's formula yields

$$\begin{aligned}
\dim \mathbb{V} &= \dim \mathbb{V}_{k-1}^{L^2}(\mathbf{r}_2; \mathbb{R}^2) + \dim \mathbb{V}_{k+2}^{\text{curl}}(\mathbf{r}_1 + 2) - 3 \\
&= \dim \mathbb{V}_{k-1}^{L^2}(\mathbf{r}_2; \mathbb{R}^2) + \dim \text{Air } \mathbb{V}_{k+2}^{\text{curl}}(\mathbf{r}_1 + 2).
\end{aligned}$$

On the other side, by the exactness of complex (55),

$$\dim \mathbb{V}_k^{\text{div}}(\mathbf{r}_1, \mathbf{r}_2; \mathbb{S}) = \dim \mathbb{V}_{k-1}^{L^2}(\mathbf{r}_2; \mathbb{R}^2) + \dim \text{Air } \mathbb{V}_{k+2}^{\text{curl}}(\mathbf{r}_1 + 2).$$

Therefore $\dim \mathbb{V}_k^{\text{div}}(\mathbf{r}_1, \mathbf{r}_2; \mathbb{S}) = \dim \mathbb{V}$. \square

Example 5.5. The pair, for $k \geq 5$, which is necessary to ensure $\mathbb{P}_1 \subseteq \overset{\circ}{\mathbb{P}}_{k-1-3(r_2^v+1)}(\mathbf{r}_2)$,

$$\mathbb{V}_k^{\text{div}}\left(\left(\begin{smallmatrix} 0 \\ -1 \end{smallmatrix}\right), \left(\begin{smallmatrix} 0 \\ 0 \end{smallmatrix}\right); \mathbb{S}\right) \xrightarrow{\text{div}} \text{Lagrange}_{k-1}\left(\left(\begin{smallmatrix} 0 \\ 0 \end{smallmatrix}\right); \mathbb{R}^2\right)$$

can be used to discretize the linear elasticity in the mixed form. The space for the symmetric stress is Hu-Zhang element with constraint $\text{div } \boldsymbol{\sigma}$ continuous at vertices and edges. The displacement space is continuous. The obtained saddle point system will have smaller dimension compared with the Hu-Zhang element and discontinuous displacement pair.

5.3. Finite element divdiv complexes. In this subsection, we consider the case: the tensor finite element space is continuous. Let $\mathbf{r}_1 \geq 0$ and $\mathbf{r}_2 \geq \max\{\mathbf{r}_1 - 2, -1\}$. We introduce the space $\mathbb{V}_k^{\text{div div}^+}(\mathbf{r}_1, \mathbf{r}_2; \mathbb{M}) \subseteq \mathbb{V}_k^{\text{div}}(\mathbf{r}_1) \times \mathbb{V}_k^{\text{div}}(\mathbf{r}_1)$ with constraint on $\text{div div } \boldsymbol{\tau}$.

The shape function space is $\mathbb{P}_k(T; \mathbb{M})$ with $k \geq \max\{2r_1^v + 3, 2r_2^v + 3\}$ and DoFs are

$$(63) \quad \nabla^i \boldsymbol{\tau}(\mathbf{v}), \quad \mathbf{v} \in \Delta_0(T), i = 0, \dots, r_1^v,$$

$$(64) \quad \nabla^j \operatorname{div} \operatorname{div} \boldsymbol{\tau}(\mathbf{v}), \quad \mathbf{v} \in \Delta_0(T), j = \max\{r_1^v - 1, 0\}, \dots, r_2^v,$$

$$(65) \quad \int_e \boldsymbol{\tau} \mathbf{n} \cdot \mathbf{q} \, ds, \quad \mathbf{q} \in \mathbb{P}_{k-2(r_1^v+1)}^2(e), e \in \Delta_1(T),$$

$$(66) \quad \int_e \partial_n^i(\boldsymbol{\tau} \mathbf{t}) \cdot \mathbf{q} \, ds, \quad \mathbf{q} \in \mathbb{P}_{k-2(r_1^v+1)+i}^2(e), e \in \Delta_1(T), i = 0, \dots, r_1^e,$$

$$(67) \quad \int_e \mathbf{n}^\top \operatorname{div} \boldsymbol{\tau} \mathbf{q} \, ds, \quad \mathbf{q} \in \mathbb{P}_{k-1-2r_1^v}(e), e \in \Delta_1(T),$$

$$(68) \quad \int_e \partial_n^i(\mathbf{t}^\top \operatorname{div} \boldsymbol{\tau}) \mathbf{q} \, ds, \quad \mathbf{q} \in \mathbb{P}_{k-1-2r_1^v+i}(e), e \in \Delta_1(T), i = 0, \dots, r_1^e - 1,$$

$$(69) \quad \int_e \partial_n^i(\operatorname{div} \operatorname{div} \boldsymbol{\tau}) \mathbf{q} \, ds, \quad \mathbf{q} \in \mathbb{P}_{k-2-2(r_2^v+1)+i}(e), e \in \Delta_1(T), i = 0, \dots, r_2^e,$$

$$(70) \quad \int_T \operatorname{div} \boldsymbol{\tau} \cdot \mathbf{q} \, dx, \quad \mathbf{q} \in \operatorname{curl} \mathbb{B}_k(\mathbf{r}_1),$$

$$(71) \quad \int_T \operatorname{div} \operatorname{div} \boldsymbol{\tau} \mathbf{q} \, dx, \quad \mathbf{q} \in \mathbb{B}_{k-2}(\mathbf{r}_2) / \mathbb{P}_1(T),$$

$$(72) \quad \int_T \boldsymbol{\tau} \cdot \mathbf{q} \, dx, \quad \mathbf{q} \in \operatorname{curl} \mathbb{B}_{k+1}(\mathbf{r}_1 + 1; \mathbb{R}^2).$$

Lemma 5.6. *Assume $k \geq \max\{2r_1^v + 3, 2r_2^v + 3\}$ and $\dim \mathbb{B}_{k-2}(\mathbf{r}_2) \geq 3$. The DoFs (63)-(72) are uni-solvent for $\mathbb{P}_k(T; \mathbb{M})$.*

Proof. The number of DoFs (64), (69) and (71) is

$$\dim \mathbb{P}_{k-2}(T) - 3 - 3 \binom{r_1^v}{2} = 3 \sum_{i=1}^{r_1^e-1} (k - 2r_1^v + i) + \dim \mathbb{B}_{k-2}(\max\{\mathbf{r}_1 - 2, -1\}) - 3.$$

And the number of DoFs (42)-(48) for $\mathbb{V}_k^{\operatorname{div}}(\mathbf{r}_1, \mathbf{r}_1 - 1)$ minus the number of DoFs (63), (65)-(68), (70) and (72) is

$$\begin{aligned} & 3 \sum_{i=1}^{r_1^e-1} (k - 2r_1^v + i) + 2 \dim \mathbb{B}_{k-1}(\mathbf{r}_1 - 1) - \dim \mathbb{B}_k(\mathbf{r}_1) - 2 \\ &= 2 \dim \mathbb{P}_{k-1}(T) - \dim \mathbb{P}_k(T) - 6 \binom{r_1^v + 1}{2} + 3 \binom{r_1^v + 2}{2} - 6 \sum_{i=0}^{r_1^e-1} (k - 2r_1^v + i) \\ & \quad + 3 \sum_{i=0}^{r_1^e} (k - 2r_1^v - 1 + i) + 3 \sum_{i=1}^{r_1^e-1} (k - 2r_1^v + i) - 2 \\ &= 2 \dim \mathbb{P}_{k-1}(T) - \dim \mathbb{P}_k(T) - 3 \binom{r_1^v}{2} - 2, \end{aligned}$$

by (9), which equals to $\dim \mathbb{P}_{k-2}(T) - 3 - 3 \binom{r_1^v}{2}$. Hence the number of DoFs (63)-(72) equals to $\dim \mathbb{P}_k(T; \mathbb{M})$.

Take $\boldsymbol{\tau} \in \mathbb{P}_k(T; \mathbb{M})$, and assume all the DoFs (63)-(72) vanish. Let $\mathbf{v} = \operatorname{div} \boldsymbol{\tau} \in \mathbb{P}_{k-1}(T; \mathbb{R}^2)$. Applying the integration by parts, it follows from (65) and (67) that

$$(\operatorname{div} \mathbf{v}, q)_T = (\operatorname{div} \operatorname{div} \boldsymbol{\tau}, q)_T = 0 \quad \forall q \in \mathbb{P}_1(T).$$

Applying Lemma 4.8, i.e. the unsolvence of space $\mathbb{V}_{k-1}^{\text{div}}(\mathbf{r}_1 - 1, \mathbf{r}_2)$, it follows from DoFs (63)-(64) and (67)-(71) that $\text{div } \boldsymbol{\tau} = \mathbf{v} = \mathbf{0}$. Then $\boldsymbol{\tau} = \text{curl } \mathbf{w}$ with some $\mathbf{w} \in \mathbb{P}_{k+1}(T; \mathbb{R}^2)$. Thanks to Theorem 3.6, we derive $\mathbf{w} = \mathbf{0}$ and $\boldsymbol{\tau} = \mathbf{0}$ from DoFs (63), (65)-(66) and (72). \square

Define global $H(\text{div div})$ -conforming finite element space

$$\mathbb{V}_k^{\text{div div}^+}(\mathbf{r}_1, \mathbf{r}_2; \mathbb{M}) = \{ \boldsymbol{\tau} \in \mathbf{L}^2(\Omega; \mathbb{M}) : \boldsymbol{\tau}|_T \in \mathbb{P}_k(T; \mathbb{M}) \forall T \in \mathcal{T}_h, \\ \text{all the DoFs (63)-(69) are single-valued} \}.$$

The super-script in div div^+ indicates the smoothness is more than div div -conforming. Indeed we have $\mathbb{V}_k^{\text{div div}^+}(\mathbf{r}_1, \mathbf{r}_2; \mathbb{M}) \subset \mathbf{H}(\text{div}, \Omega; \mathbb{M}) \cap \mathbf{H}(\text{div div}, \Omega; \mathbb{M})$.

Theorem 5.7. *Let $\mathbf{r}_1 \geq 0$ and $\mathbf{r}_2 \geq \max\{\mathbf{r}_1 - 2, -1\}$. Assume $k \geq \max\{2r_1^v + 3, 2r_2^v + 3\}$ and $\dim \mathbb{B}_{k-2}(\mathbf{r}_2) \geq 3$. The BGG diagram*

$$(73) \quad \begin{array}{ccccccc} \mathbb{R}^2 & \xhookrightarrow{\subset} & \mathbb{V}_{k+1}^{\text{curl}}(\mathbf{r}_1 + 1; \mathbb{R}^2) & \xrightarrow{\text{curl}} & \mathbb{V}_k^{\text{div div}^+}(\mathbf{r}_1, \mathbf{r}_2; \mathbb{M}) & \xrightarrow{\text{div}} & \mathbb{V}_{k-1}^{\text{div}}(\mathbf{r}_1 - 1, \mathbf{r}_2) \rightarrow \mathbf{0} \\ & & \nearrow \text{mskw} & & \nearrow \text{id} & & \\ \mathbb{R} & \xhookrightarrow{\subset} & \mathbb{V}_k^{\text{curl}}(\mathbf{r}_1) & \xrightarrow{\text{curl}} & \mathbb{V}_{k-1}^{\text{div}}(\mathbf{r}_1 - 1, \mathbf{r}_2) & \xrightarrow{\text{div}} & \mathbb{V}_{k-2}^{L^2}(\mathbf{r}_2) \longrightarrow \mathbf{0} \end{array}$$

which leads to the finite element div div complex

$$(74) \quad \mathbf{RT} \xhookrightarrow{\subset} \mathbb{V}_{k+1}^{\text{curl}}(\mathbf{r}_1 + 1; \mathbb{R}^2) \xrightarrow{\text{sym curl}} \mathbb{V}_k^{\text{div div}^+}(\mathbf{r}_1, \mathbf{r}_2; \mathbb{S}) \xrightarrow{\text{div div}} \mathbb{V}_{k-2}^{L^2}(\mathbf{r}_2) \rightarrow \mathbf{0},$$

where $\mathbb{V}_k^{\text{div div}^+}(\mathbf{r}_1, \mathbf{r}_2; \mathbb{S}) := \mathbb{V}_k^{\text{div div}^+}(\mathbf{r}_1, \mathbf{r}_2; \mathbb{M}) / \text{mskw } \mathbb{V}_k^{\text{curl}}(\mathbf{r}_1)$.

Proof. By the anti-commutative property $\text{div}(\text{mskw } v) = -\text{curl } v$, we can conclude complex (74) from the BGG framework in [7].

In the following we give a self-contained proof without invoking the BGG framework. Clearly (74) is a complex. As $\text{div div mskw } \mathbb{V}_k^{\text{curl}}(\mathbf{r}_1) = -\text{div curl } \mathbb{V}_k^{\text{curl}}(\mathbf{r}_1) = 0$, we have

$$\text{div div } \mathbb{V}_k^{\text{div div}^+}(\mathbf{r}_1, \mathbf{r}_2; \mathbb{S}) = \text{div div } \mathbb{V}_k^{\text{div div}^+}(\mathbf{r}_1, \mathbf{r}_2; \mathbb{M}) = \mathbb{V}_{k-2}^{L^2}(\mathbf{r}_2).$$

By two complexes in diagram (73), we have

$$\dim \mathbb{V}_k^{\text{div div}^+}(\mathbf{r}_1, \mathbf{r}_2; \mathbb{M}) = \dim \mathbb{V}_{k+1}^{\text{curl}}(\mathbf{r}_1 + 1; \mathbb{R}^2) + \dim \mathbb{V}_{k-1}^{\text{div}}(\mathbf{r}_1 - 1, \mathbf{r}_2) - 2, \\ \dim \mathbb{V}_{k-1}^{\text{div}}(\mathbf{r}_1 - 1, \mathbf{r}_2) = \dim \mathbb{V}_k^{\text{curl}}(\mathbf{r}_1) + \dim \mathbb{V}_{k-2}^{L^2}(\mathbf{r}_2) - 1.$$

Combining the last two equations yields

$$\dim \mathbb{V}_k^{\text{div div}^+}(\mathbf{r}_1, \mathbf{r}_2; \mathbb{M}) = \dim \mathbb{V}_{k+1}^{\text{curl}}(\mathbf{r}_1 + 1; \mathbb{R}^2) + \dim \mathbb{V}_k^{\text{curl}}(\mathbf{r}_1) + \dim \mathbb{V}_{k-2}^{L^2}(\mathbf{r}_2) - 3.$$

Hence

$$\dim \mathbb{V}_k^{\text{div div}^+}(\mathbf{r}_1, \mathbf{r}_2; \mathbb{S}) = \dim \mathbb{V}_{k+1}^{\text{curl}}(\mathbf{r}_1 + 1; \mathbb{R}^2) + \dim \mathbb{V}_{k-2}^{L^2}(\mathbf{r}_2) - 3.$$

Therefore the exactness of complex (74) follows from Lemma 2.1. \square

Next we give the finite element characterization of $\mathbb{V}_k^{\text{div div}^+}(\mathbf{r}_1, \mathbf{r}_2; \mathbb{S})$. We choose $\mathbb{P}_k(T; \mathbb{S})$ as the shape function space. By symmetrizing DoFs (63)-(72), we propose the

following local DoFs:

$$(75) \quad \nabla^i \boldsymbol{\tau}(\mathbf{v}), \quad \mathbf{v} \in \Delta_0(T), i = 0, \dots, r_1^v,$$

$$(76) \quad \nabla^j \operatorname{div} \operatorname{div} \boldsymbol{\tau}(\mathbf{v}), \quad \mathbf{v} \in \Delta_0(T), j = \max\{r_1^v - 1, 0\}, \dots, r_2^v,$$

$$(77) \quad \int_e \boldsymbol{\tau} \mathbf{n} \cdot \mathbf{q} \, ds, \quad \mathbf{q} \in \mathbb{P}_{k-2}^2(r_1^v+1)(e), e \in \Delta_1(T),$$

$$(78) \quad \int_e \partial_n^i(\mathbf{t}^\top \boldsymbol{\tau} \mathbf{t}) q \, ds, \quad q \in \mathbb{P}_{k-2}(r_1^v+1)_i(e), e \in \Delta_1(T), i = 0, \dots, r_1^e,$$

$$(79) \quad \int_e \mathbf{n}^\top \operatorname{div} \boldsymbol{\tau} q \, ds, \quad q \in \mathbb{P}_{k-1-2r_1^v}(e), e \in \Delta_1(T),$$

$$(80) \quad \int_e \partial_n^i(\mathbf{t}^\top \operatorname{div} \boldsymbol{\tau}) q \, ds, \quad q \in \mathbb{P}_{k-1-2r_1^v+i}(e), e \in \Delta_1(T), i = 0, \dots, r_1^e - 1,$$

$$(81) \quad \int_e \partial_n^i(\operatorname{div} \operatorname{div} \boldsymbol{\tau}) q \, ds, \quad q \in \mathbb{P}_{k-2}(r_2^v+2)_i(e), e \in \Delta_1(T), i = 0, \dots, r_2^e,$$

$$(82) \quad \int_T \operatorname{div} \boldsymbol{\tau} \cdot \mathbf{q} \, dx, \quad \mathbf{q} \in \operatorname{curl} \mathbb{B}_k(\mathbf{r}_1)/\mathbf{x}^\perp,$$

$$(83) \quad \int_T \operatorname{div} \operatorname{div} \boldsymbol{\tau} q \, dx, \quad q \in \mathbb{B}_{k-2}(\mathbf{r}_2)/\mathbb{P}_1(T),$$

$$(84) \quad \int_T \boldsymbol{\tau} \cdot \mathbf{q} \, dx, \quad \mathbf{q} \in \operatorname{Air} \mathbb{B}_{k+2}(\mathbf{r}_1 + 2).$$

Lemma 5.8. *Let $r_1 \geq 0$ and $r_2 \geq \max\{r_1 - 2, -1\}$. Assume $k \geq \max\{2r_1^v + 3, 2r_2^v + 3\}$ and $\dim \mathbb{B}_{k-2}(\mathbf{r}_2) \geq 3$. The DoFs (75)-(84) are uni-solvent for $\mathbb{P}_k(T; \mathbb{S})$.*

Proof. By complex (32),

$$\dim \mathbb{B}_{k+1}(\mathbf{r}_1 + 1; \mathbb{R}^2) = \dim \mathbb{B}_{k+2}(\mathbf{r}_1 + 2) + \dim \mathbb{B}_k(\mathbf{r}_1) - 1.$$

Then the difference between the numbers of DoFs (63)-(72) and DoFs (75)-(84)

$$3 \binom{r_1^e + 2}{2} + 3 \sum_{i=0}^{r_1^e} (k - 1 - 2r_1^v + i) + 1 + \dim \mathbb{B}_{k+1}(\mathbf{r}_1 + 1; \mathbb{R}^2) - \dim \mathbb{B}_{k+2}(\mathbf{r}_1 + 2)$$

equals to $\dim \mathbb{P}_k(T)$. Hence the number of DoFs (75)-(84) equals to $\dim \mathbb{P}_k(T; \mathbb{S})$.

Take $\boldsymbol{\tau} \in \mathbb{P}_k(T; \mathbb{S})$, and assume all the DoFs (75)-(84) vanish. Let $\mathbf{v} = \operatorname{div} \boldsymbol{\tau} \in \mathbb{P}_{k-1}(T; \mathbb{R}^2)$. Applying the integration by parts, we get from (77) and (79) that

$$(\mathbf{v}, \mathbf{x}^\perp)_T = (\operatorname{div} \boldsymbol{\tau}, \mathbf{x}^\perp)_T = 0, \quad (\operatorname{div} \mathbf{v}, q)_T = (\operatorname{div} \operatorname{div} \boldsymbol{\tau}, q)_T = 0 \quad \forall q \in \mathbb{P}_1(T).$$

Applying Lemma 4.8, i.e. the unisolvence of space $\mathbb{V}_{k-1}^{\operatorname{div}}(\mathbf{r}_1 - 1, \mathbf{r}_2)$, it follows from DoFs (75)-(76) and (79)-(83) that $\operatorname{div} \boldsymbol{\tau} = \mathbf{v} = \mathbf{0}$. Finally, applying Lemma 5.3, $\boldsymbol{\tau} = \mathbf{0}$ holds from (75), (77)-(78) and (84). \square

Lemma 5.9. *Let $r_1 \geq 0$ and $r_2 \geq \max\{r_1 - 2, -1\}$. Assume $k \geq \max\{2r_1^v + 3, 2r_2^v + 3\}$ and $\dim \mathbb{B}_{k-2}(\mathbf{r}_2) \geq 3$. It holds*

$$\mathbb{V}_k^{\operatorname{div} \operatorname{div}^+}(\mathbf{r}_1, \mathbf{r}_2; \mathbb{S}) = \mathbb{V} := \{\boldsymbol{\tau} \in \mathbf{L}^2(\Omega; \mathbb{S}) : \boldsymbol{\tau}|_T \in \mathbb{P}_k(T; \mathbb{S}) \forall T \in \mathcal{T}_h, \\ \text{all the DoFs (75)-(81) are single-valued}\}$$

and $\mathbb{V}_k^{\operatorname{div} \operatorname{div}^+}(\mathbf{r}_1, \mathbf{r}_2; \mathbb{S}) \subset \mathbf{H}(\operatorname{div}, \Omega; \mathbb{S}) \cap \mathbf{H}(\operatorname{div} \operatorname{div}, \Omega; \mathbb{S})$.

Proof. Apparently $\mathbb{V} \subseteq \mathbb{V}_k^{\text{div div}^+}(\mathbf{r}_1, \mathbf{r}_2; \mathbb{S})$. It suffices to prove $\dim \mathbb{V}_k^{\text{div div}^+}(\mathbf{r}_1, \mathbf{r}_2; \mathbb{S}) = \dim \mathbb{V}$. By comparing DoFs and direct computation,

$$\begin{aligned}
& \dim \mathbb{V} - \dim \mathbb{V}_{k-2}^{L^2}(\mathbf{r}_2) \\
&= 3 \binom{r_1^v + 2}{2} |\Delta_0(\mathcal{T}_h)| - \binom{r_1^v}{2} |\Delta_0(\mathcal{T}_h)| + (2k - 2 - 4r_1^v - r_1^e) |\Delta_1(\mathcal{T}_h)| \\
&\quad + |\Delta_1(\mathcal{T}_h)| \sum_{i=0}^{r_1^e} (2k - 1 - 4r_1^v + 2i) \\
&\quad + |\Delta_2(\mathcal{T}_h)| (\dim \mathbb{B}_k(\mathbf{r}_1) + \dim \mathbb{B}_{k+2}(\mathbf{r}_1 + 2) - 4) \\
&= 2 |\Delta_0(\mathcal{T}_h)| \binom{r_1^v + 3}{2} + 2 |\Delta_1(\mathcal{T}_h)| (r_1^e + 2) (k - 2r_1^v - 3/2 + r_1^e/2) \\
&\quad + 2 |\Delta_2(\mathcal{T}_h)| \dim \mathbb{B}_{k+1}(\mathbf{r}_1 + 1) - 3 (|\Delta_0(\mathcal{T}_h)| - |\Delta_1(\mathcal{T}_h)| + |\Delta_2(\mathcal{T}_h)|) \\
&= \dim \mathbb{V}_{k+1}^{\text{curl}}(\mathbf{r}_1 + 1; \mathbb{R}^2) - 3 (|\Delta_0(\mathcal{T}_h)| - |\Delta_1(\mathcal{T}_h)| + |\Delta_2(\mathcal{T}_h)|),
\end{aligned}$$

which together with the Euler's formula yields

$$\begin{aligned}
\dim \mathbb{V} &= \dim \mathbb{V}_{k-2}^{L^2}(\mathbf{r}_2) + \dim \mathbb{V}_{k+1}^{\text{curl}}(\mathbf{r}_1 + 1; \mathbb{R}^2) - 3 \\
&= \dim \mathbb{V}_{k-2}^{L^2}(\mathbf{r}_2) + \dim \text{sym curl } \mathbb{V}_{k+1}^{\text{curl}}(\mathbf{r}_1 + 1; \mathbb{R}^2).
\end{aligned}$$

On the other side, by complex (74),

$$\dim \mathbb{V}_k^{\text{div div}^+}(\mathbf{r}_1, \mathbf{r}_2; \mathbb{S}) = \dim \mathbb{V}_{k-2}^{L^2}(\mathbf{r}_2) + \dim \text{sym curl } \mathbb{V}_{k+1}^{\text{curl}}(\mathbf{r}_1 + 1; \mathbb{R}^2).$$

Therefore $\dim \mathbb{V}_k^{\text{div div}^+}(\mathbf{r}_1, \mathbf{r}_2; \mathbb{S}) = \dim \mathbb{V}$. \square

Remark 5.10. We assume $\mathbf{r}_1 \geq 0$ and thus $\tau|_e$ is continuous. Then through linear combination DoF (79) can be replaced by

$$\int_e \text{tr}_2^{\text{div div}}(\boldsymbol{\tau}) q \, ds, \quad q \in \mathbb{P}_{k-1-2r_1^v}(e),$$

where $\text{tr}_2^{\text{div div}}(\boldsymbol{\tau}) = \partial_t(\mathbf{t}^\top \boldsymbol{\tau} \mathbf{n}) + \mathbf{n}^\top \text{div } \boldsymbol{\tau}$ is one of the trace operators of div div ; see [14].

Example 5.11. We choose $\mathbf{r}_1 = (1, 0)$, $\mathbf{r}_2 = (0, 0)$ to get the div div complex constructed in [15]

$$\mathbf{RT} \xrightarrow{\subset} \text{Argy} \left(\binom{2}{1}; \mathbb{R}^2 \right) \xrightarrow{\text{sym curl}} \mathbb{V}_k^{\text{div div}^+} \left(\binom{1}{0}, \binom{0}{0}; \mathbb{S} \right) \xrightarrow{\text{div div}} \text{Lagrange}_{k-2} \left(\binom{0}{0} \right) \rightarrow 0.$$

5.4. Out of BGG construction. The BGG framework can only change the algebraic structure but not the smoothness of the Sobolev spaces. In this subsection we provide two examples for finite element div div complex not using the BGG framework.

Consider the case $\mathbf{r}_1 = (r_1^v, -1)$, $r_1^v \geq 0$ and $\mathbf{r}_2 \geq \max\{\mathbf{r}_1 - 2, -1\}$. We still have the BGG diagram

$$\begin{array}{ccccc}
\mathbb{V}_{k+1}^{\text{curl}} \left(\binom{r_1^v + 1}{0}; \mathbb{R}^2 \right) & \xrightarrow{\text{curl}} & \mathbb{V}_k^{\text{div div}^+} \left(\binom{r_1^v}{-1}, \mathbf{r}_2; \mathbb{M} \right) & \xrightarrow{\text{div}} & \mathbb{V}_{k-1}^{\text{div}} \left(\binom{r_1^v - 1}{-1}, \mathbf{r}_2 \right) \\
(85) & \nearrow \text{mskw} & & \nearrow \text{id} & \\
\mathbb{V}_k^{\text{curl}} \left(\binom{r_1^v}{0} \right) & \xrightarrow{\text{curl}} & \mathbb{V}_{k-1}^{\text{div}} \left(\binom{r_1^v - 1}{-1}, \mathbf{r}_2 \right) & \xrightarrow{\text{div}} & \mathbb{V}_{k-2}^{L^2}(\mathbf{r}_2)
\end{array}$$

But this case cannot be included in the previous theorem, since now $\text{sskw}(\boldsymbol{\tau})$ is discontinuous for $\boldsymbol{\tau} \in \mathbb{V}_k^{\text{div}}\left(\begin{pmatrix} r_1^\vee \\ -1 \end{pmatrix}, \mathbf{r}_2; \mathbb{M}\right)$. The operator mskw is still injective. But it is unclear if $\mathbb{V}_k^{\text{div div}^+}\left(\begin{pmatrix} r_1^\vee \\ -1 \end{pmatrix}, \mathbf{r}_2; \mathbb{M}\right) / \text{mskw} \mathbb{V}_k^{\text{curl}}\left(\begin{pmatrix} r_1^\vee \\ 0 \end{pmatrix}\right)$ consists of symmetric matrix functions with desirable normal continuity.

We present a divdiv complex where $\mathbf{H}^1(\Omega; \mathbb{R}^2)$ is replaced by subspace $\mathbf{H}^1(\text{div}, \Omega)$.

Lemma 5.12. *The divdiv complex*

$$(86) \quad \mathbf{RT} \xrightarrow{\subset} \mathbf{H}^1(\text{div}, \Omega) \xrightarrow{\text{sym curl}} \mathbf{H}(\text{divdiv}, \Omega; \mathbb{S}) \cap \mathbf{H}(\text{div}, \Omega; \mathbb{S}) \xrightarrow{\text{divdiv}} L^2(\Omega) \rightarrow 0$$

is exact, where $\mathbf{H}^1(\text{div}, \Omega) := \{\mathbf{v} \in \mathbf{H}^1(\Omega; \mathbb{R}^2) : \text{div } \mathbf{v} \in H^1(\Omega)\}$.

Proof. Clearly (86) is a complex. We will show the exactness of complex (86).

By Theorem 1.1 in [21], we have $\text{div div } \mathbf{H}^2(\Omega; \mathbb{S}) = \text{div div } \mathbf{H}^2(\Omega; \mathbb{M}) = L^2(\Omega)$. Thanks to $\text{div div } \mathbf{H}^2(\Omega; \mathbb{S}) \subseteq \text{div div } (\mathbf{H}(\text{divdiv}, \Omega; \mathbb{S}) \cap \mathbf{H}(\text{div}, \Omega; \mathbb{S})) \subseteq L^2(\Omega)$, we acquire $\text{div div } (\mathbf{H}(\text{divdiv}, \Omega; \mathbb{S}) \cap \mathbf{H}(\text{div}, \Omega; \mathbb{S})) = L^2(\Omega)$.

Next we prove

$$(\mathbf{H}(\text{div div}, \Omega; \mathbb{S}) \cap \mathbf{H}(\text{div}, \Omega; \mathbb{S})) \cap \ker(\text{div div}) = \text{sym curl } \mathbf{H}^1(\text{div}, \Omega; \mathbb{R}^2).$$

For $\boldsymbol{\tau} \in (\mathbf{H}(\text{div div}, \Omega; \mathbb{S}) \cap \mathbf{H}(\text{div}, \Omega; \mathbb{S})) \cap \ker(\text{div div})$, by the standard divdiv complex, there exists $\mathbf{v} \in \mathbf{H}^1(\Omega; \mathbb{R}^2)$ such that $\boldsymbol{\tau} = \text{sym curl } \mathbf{v}$. Since

$$\text{div } \boldsymbol{\tau} = \frac{1}{2} \text{curl}(\text{div } \mathbf{v}) \in \mathbf{L}^2(\Omega; \mathbb{R}^2),$$

we get $\text{div } \mathbf{v} \in H^1(\Omega)$. Thus $\mathbf{v} \in \mathbf{H}^1(\text{div}, \Omega; \mathbb{R}^2)$. \square

For $\mathbf{r}_1 = (r_1^\vee, -1)$, $r_1^\vee \geq 0$, we propose the following DoFs for space $\mathbb{V}_k^{\text{div div}^+}(\mathbf{r}_1, \mathbf{r}_2; \mathbb{S})$

$$(87) \quad \nabla^i \boldsymbol{\tau}(\mathbf{v}), \quad \mathbf{v} \in \Delta_0(T), i = 0, \dots, r_1^\vee,$$

$$(88) \quad \nabla^j \text{div div } \boldsymbol{\tau}(\mathbf{v}), \quad \mathbf{v} \in \Delta_0(T), j = \max\{r_1^\vee - 1, 0\}, \dots, r_2^\vee,$$

$$(89) \quad \int_e \boldsymbol{\tau} \mathbf{n} \cdot \mathbf{q} \, ds, \quad \mathbf{q} \in \mathbb{P}_{k-2(r_1^\vee+1)}^2(e), e \in \Delta_1(T),$$

$$(90) \quad \int_e \mathbf{n}^\top \text{div } \boldsymbol{\tau} \mathbf{q} \, ds, \quad \mathbf{q} \in \mathbb{P}_{k-1-2r_1^\vee}(e), e \in \Delta_1(T),$$

$$(91) \quad \int_e \partial_n^i(\text{div div } \boldsymbol{\tau}) \mathbf{q} \, ds, \quad \mathbf{q} \in \mathbb{P}_{k-2(r_2^\vee+2)+i}(e), e \in \Delta_1(T), i = 0, \dots, r_2^e,$$

$$(92) \quad \int_T \text{div } \boldsymbol{\tau} \cdot \mathbf{q} \, dx, \quad \mathbf{q} \in \text{curl } \mathbb{B}_k\left(\begin{pmatrix} r_1^\vee \\ 0 \end{pmatrix}\right) / \mathbf{x}^\perp,$$

$$(93) \quad \int_T \text{div div } \boldsymbol{\tau} \mathbf{q} \, dx, \quad \mathbf{q} \in \mathbb{B}_{k-2}(\mathbf{r}_2) / \mathbb{P}_1(T),$$

$$(94) \quad \int_T \boldsymbol{\tau} \cdot \mathbf{q} \, dx, \quad \mathbf{q} \in \text{Air } \mathbb{B}_{k+2}(\mathbf{r}_1 + 2).$$

Lemma 5.13. *Let $\mathbf{r}_1 = (r_1^\vee, -1)$, $r_1^\vee \geq 0$ and $\mathbf{r}_2 \geq \max\{\mathbf{r}_1 - 2, -1\}$. Assume $k \geq \max\{2r_1^\vee + 3, 2r_2^\vee + 3\}$ and $\dim \mathbb{B}_{k-2}(\mathbf{r}_2) \geq 3$. The DoFs (87)-(94) are uni-solvent for $\mathbb{P}_k(T; \mathbb{S})$.*

Proof. The difference between the numbers of DoFs (75)-(84) with $\mathbf{r}_1 = (r_1^v, 0)$ and DoFs (87)-(94)

$$3(k-1-2r_1^v) + \dim \mathbb{B}_{k+2}\left(\begin{pmatrix} r_1^v+2 \\ 2 \end{pmatrix}\right) - \dim \mathbb{B}_{k+2}\left(\begin{pmatrix} r_1^v+2 \\ 1 \end{pmatrix}\right) = 0.$$

Hence the number of DoFs (87)-(94) equals to $\dim \mathbb{P}_k(T; \mathbb{S})$.

Take $\boldsymbol{\tau} \in \mathbb{P}_k(T; \mathbb{S})$, and assume all the DoFs (87)-(94) vanish. Applying the integration by parts, we get from (89)-(90) that

$$(\operatorname{div} \operatorname{div} \boldsymbol{\tau}, q)_T = 0 \quad \forall q \in \mathbb{P}_1(T).$$

Then it follows from DoFs (87)-(88), (91) and (93) that $\operatorname{div} \operatorname{div} \boldsymbol{\tau} = 0$. Let $\mathbf{v} = \operatorname{div} \boldsymbol{\tau} \in \mathbb{P}_{k-1}(T; \mathbb{R}^2)$. Applying the integration by parts, we get from (89) that

$$(\mathbf{v}, \mathbf{x}^\perp)_T = (\operatorname{div} \boldsymbol{\tau}, \mathbf{x}^\perp)_T = 0.$$

Applying Lemma 4.8, i.e. the unsolvence of $\mathbb{V}_{k-1}^{\operatorname{div}}\left(\begin{pmatrix} r_1^v-1 \\ -1 \end{pmatrix}, \begin{pmatrix} \max\{r_1^v-2, -1\} \\ -1 \end{pmatrix}\right)$, it follows from DoFs (87), (90) and (92) that $\operatorname{div} \boldsymbol{\tau} = \mathbf{v} = \mathbf{0}$. Finally, applying Lemma 5.3, $\boldsymbol{\tau} = \mathbf{0}$ holds from (87), (89) and (94). \square

Theorem 5.14. *Let $\mathbf{r}_1 = (r_1^v, -1)$, $r_1^v \geq 0$ and $\mathbf{r}_2 \geq \max\{r_1 - 2, -1\}$. Assume $k \geq \max\{2r_1^v+3, 2r_2^v+3\}$ and $\dim \mathbb{B}_{k-2}(\mathbf{r}_2) \geq 3$. The following finite element divdiv complex is exact*

$$(95) \quad \mathbf{RT} \xrightarrow{\subset} \mathbb{V}_{k+1}^{\operatorname{div}}\left(\begin{pmatrix} r_1^v+1 \\ 0 \end{pmatrix}, \begin{pmatrix} r_1^v \\ 0 \end{pmatrix}\right) \xrightarrow{\operatorname{sym} \operatorname{curl}} \mathbb{V}_k^{\operatorname{div} \operatorname{div}^+}\left(\begin{pmatrix} r_1^v \\ -1 \end{pmatrix}, \mathbf{r}_2; \mathbb{S}\right) \xrightarrow{\operatorname{div} \operatorname{div}} \mathbb{V}_{k-2}^{L^2}(\mathbf{r}_2) \rightarrow 0.$$

Proof. It is easy to check that (95) is a complex. We will prove the exactness of complex (95).

By divdiv complex (74), we have $\operatorname{div} \operatorname{div} \mathbb{V}_k^{\operatorname{div} \operatorname{div}^+}\left(\begin{pmatrix} r_1^v \\ -1 \end{pmatrix}, \mathbf{r}_2; \mathbb{S}\right) = \mathbb{V}_{k-2}^{L^2}(\mathbf{r}_2)$. Noting that

$$\operatorname{div} \operatorname{div} \mathbb{V}_k^{\operatorname{div} \operatorname{div}^+}\left(\begin{pmatrix} r_1^v \\ 0 \end{pmatrix}, \mathbf{r}_2; \mathbb{S}\right) \subseteq \operatorname{div} \operatorname{div} \mathbb{V}_k^{\operatorname{div} \operatorname{div}^+}\left(\begin{pmatrix} r_1^v \\ -1 \end{pmatrix}, \mathbf{r}_2; \mathbb{S}\right) \subseteq \mathbb{V}_{k-2}^{L^2}(\mathbf{r}_2),$$

hence $\operatorname{div} \operatorname{div} \mathbb{V}_k^{\operatorname{div} \operatorname{div}^+}\left(\begin{pmatrix} r_1^v \\ -1 \end{pmatrix}, \mathbf{r}_2; \mathbb{S}\right) = \mathbb{V}_{k-2}^{L^2}(\mathbf{r}_2)$. On the other side,

$$\begin{aligned} & \dim \mathbb{V}_k^{\operatorname{div} \operatorname{div}^+}\left(\begin{pmatrix} r_1^v \\ -1 \end{pmatrix}, \mathbf{r}_2; \mathbb{S}\right) - \dim \mathbb{V}_{k-2}^{L^2}(\mathbf{r}_2) \\ &= 3 \binom{r_1^v+2}{2} |\Delta_0(\mathcal{T}_h)| - \binom{r_1^v}{2} |\Delta_0(\mathcal{T}_h)| + (3k - 6r_1^v - 2) |\Delta_1(\mathcal{T}_h)| \\ & \quad + |\Delta_2(\mathcal{T}_h)| \dim \mathbb{B}_k\left(\begin{pmatrix} r_1^v \\ 0 \end{pmatrix}\right) + |\Delta_2(\mathcal{T}_h)| \dim \mathbb{B}_{k+2}\left(\begin{pmatrix} r_1^v+2 \\ 1 \end{pmatrix}\right) - 4 |\Delta_2(\mathcal{T}_h)| \\ &= 2 \binom{r_1^v+3}{2} |\Delta_0(\mathcal{T}_h)| + (3k - 6r_1^v - 5) |\Delta_1(\mathcal{T}_h)| \\ & \quad + |\Delta_2(\mathcal{T}_h)| \dim \mathbb{B}_k\left(\begin{pmatrix} r_1^v \\ 0 \end{pmatrix}\right) + |\Delta_2(\mathcal{T}_h)| \dim \mathbb{B}_{k+2}\left(\begin{pmatrix} r_1^v+2 \\ 1 \end{pmatrix}\right) - |\Delta_2(\mathcal{T}_h)| \\ & \quad - 3(|\Delta_0(\mathcal{T}_h)| - |\Delta_1(\mathcal{T}_h)| + |\Delta_2(\mathcal{T}_h)|). \end{aligned}$$

Thanks to the DoFs (42)-(48) for $\mathbb{V}_{k+1}^{\text{div}}\left(\begin{pmatrix} r_1^v + 1 \\ 0 \end{pmatrix}, \begin{pmatrix} r_1^v \\ 0 \end{pmatrix}\right)$ and the Euler's formula,

$$\dim \mathbb{V}_k^{\text{div div}^+}\left(\begin{pmatrix} r_1^v \\ -1 \end{pmatrix}, \mathbf{r}_2; \mathbb{S}\right) - \dim \mathbb{V}_{k-2}^{L^2}(\mathbf{r}_2) = \dim \mathbb{V}_{k+1}^{\text{div}}\left(\begin{pmatrix} r_1^v + 1 \\ 0 \end{pmatrix}, \begin{pmatrix} r_1^v \\ 0 \end{pmatrix}\right) - 3,$$

which together with Lemma 2.1 indicates the exactness of complex (95). \square

Example 5.15. When $r_1^v = 0$ and $\mathbf{r}_2 = -1$, we recover the finite element divdiv complex constructed in [26]

$$\mathbf{RT} \xrightarrow{\subset} \mathbb{V}_{k+1}^{\text{div}}\left(\begin{pmatrix} 1 \\ 0 \end{pmatrix}, \begin{pmatrix} 0 \\ 0 \end{pmatrix}\right) \xrightarrow{\text{sym curl}} \text{HMZ}_k\left(\begin{pmatrix} 0 \\ -1 \end{pmatrix}\right) \xrightarrow{\text{div div}} \text{DG}_{k-2}\left(\begin{pmatrix} -1 \\ -1 \end{pmatrix}\right) \rightarrow 0.$$

Another modification is to relax the smoothness $\mathbf{H}(\text{div div}, \Omega; \mathbb{S}) \cap \mathbf{H}(\text{div}, \Omega; \mathbb{S})$ to $\mathbf{H}(\text{div div}, \Omega; \mathbb{S})$ only. The DoFs are given by

$$(96) \quad \nabla^i \boldsymbol{\tau}(\mathbf{v}), \quad \mathbf{v} \in \Delta_0(T), i = 0, \dots, r_1^v,$$

$$(97) \quad \nabla^j \text{div div } \boldsymbol{\tau}(\mathbf{v}), \quad \mathbf{v} \in \Delta_0(T), j = \max\{r_1^v - 1, 0\}, \dots, r_2^v,$$

$$(98) \quad \int_e \mathbf{n}^\top \boldsymbol{\tau} \mathbf{n} \cdot \mathbf{q} \, ds, \quad \mathbf{q} \in \mathbb{P}_{k-2(r_1^v+1)}(e), e \in \Delta_1(T),$$

$$(99) \quad \int_e \mathbf{t}^\top \boldsymbol{\tau} \mathbf{n} \cdot \mathbf{q} \, ds, \quad \mathbf{q} \in \mathbb{P}_{k-2(r_1^v+1)}(e), e \in \Delta_1(T),$$

$$(100) \quad \int_e \text{tr}_2^{\text{div div}}(\boldsymbol{\tau}) q \, ds, \quad q \in \mathbb{P}_{k-1-2r_1^v}(e), e \in \Delta_1(T),$$

$$(101) \quad \int_e \partial_n^i(\text{div div } \boldsymbol{\tau}) q \, ds, \quad q \in \mathbb{P}_{k-2(r_2^v+2)+i}(e), e \in \Delta_1(T), i = 0, \dots, r_2^e,$$

$$(102) \quad \int_T \text{div } \boldsymbol{\tau} \cdot \mathbf{q} \, dx, \quad \mathbf{q} \in \text{curl } \mathbb{B}_k\left(\begin{pmatrix} r_1^v \\ 0 \end{pmatrix}\right) / \mathbf{x}^\perp,$$

$$(103) \quad \int_T \text{div div } \boldsymbol{\tau} q \, dx, \quad q \in \mathbb{B}_{k-2}(\mathbf{r}_2) / \mathbb{P}_1(T),$$

$$(104) \quad \int_T \boldsymbol{\tau} \cdot \mathbf{q} \, dx, \quad \mathbf{q} \in \text{Air } \mathbb{B}_{k+2}(\mathbf{r}_1 + 2).$$

Lemma 5.16. *The DoFs (96)-(104) are uni-solvent for $\mathbb{P}_k(T; \mathbb{S})$.*

Proof. Recall that $\text{tr}_2^{\text{div div}}(\boldsymbol{\tau}) = \partial_t(\mathbf{t}^\top \boldsymbol{\tau} \mathbf{n}) + \mathbf{n}^\top \text{div } \boldsymbol{\tau}$. Then by linear combination, it will determine $\mathbf{n}^\top \text{div } \boldsymbol{\tau}$. Then the uni-solvence follows from that of Lemma 5.13. \square

Define

$$\mathbb{V}_k^{\text{div div}}\left(\begin{pmatrix} r_1^v \\ -1 \end{pmatrix}, \mathbf{r}_2; \mathbb{S}\right) = \mathbb{V} := \{\boldsymbol{\tau} \in \mathbf{L}^2(\Omega; \mathbb{S}) : \boldsymbol{\tau}|_T \in \mathbb{P}_k(T; \mathbb{S}) \forall T \in \mathcal{T}_h,$$

all the DoFs (96)-(101) except (99) are single-valued\}.

As $\mathbf{t}^\top \boldsymbol{\tau} \mathbf{n}$ is local, the vector $\boldsymbol{\tau} \mathbf{n}$ is not continuous across edges. But $\text{tr}_1^{\text{div div}}(\boldsymbol{\tau}) = \mathbf{n}^\top \boldsymbol{\tau} \mathbf{n}$ and $\text{tr}_2^{\text{div div}}(\boldsymbol{\tau})$ are continuous. So the space $\mathbb{V}_k^{\text{div div}}\left(\begin{pmatrix} r_1^v \\ -1 \end{pmatrix}, \mathbf{r}_2; \mathbb{S}\right) \subset \mathbf{H}(\text{div div}, \Omega; \mathbb{S})$ but not in $\mathbf{H}(\text{div}, \Omega; \mathbb{S})$. It cannot be derived from the BGG diagram (85) as the induced space should be in $\mathbf{H}(\text{div}, \Omega; \mathbb{S})$.

Theorem 5.17. *The following finite element divdiv complex is exact*

$$(105) \quad \mathbf{RT} \xrightarrow{\subset} \mathbb{V}_{k+1}^{\text{curl}}\left(\begin{pmatrix} r_1^v + 1 \\ 0 \end{pmatrix}; \mathbb{R}^2\right) \xrightarrow{\text{sym curl}} \mathbb{V}_k^{\text{div div}}\left(\begin{pmatrix} r_1^v \\ -1 \end{pmatrix}, \mathbf{r}_2; \mathbb{S}\right) \xrightarrow{\text{div div}} \mathbb{V}_{k-2}^{L^2}(\mathbf{r}_2) \rightarrow 0.$$

Proof. For $\boldsymbol{\tau} = \text{sym curl } \mathbf{v}$, we have [14, Lemma 2.2]

$$\mathbf{n}^\top \boldsymbol{\tau} \mathbf{n} = \partial_t(\mathbf{v} \cdot \mathbf{n}), \quad \text{tr}_2^{\text{div div}}(\boldsymbol{\tau}) = \partial_{tt}(\mathbf{v} \cdot \mathbf{t}).$$

Then it is obvious that (105) is a complex. We will show the exactness of complex (105).

Noting that $\mathbb{V}_k^{\text{div div}^+}(\begin{pmatrix} r_1^\vee \\ -1 \end{pmatrix}, \mathbf{r}_2; \mathbb{S}) \subseteq \mathbb{V}_k^{\text{div div}}(\begin{pmatrix} r_1^\vee \\ -1 \end{pmatrix}, \mathbf{r}_2; \mathbb{S})$, by the exactness of complex (95), we have

$$\text{div div } \mathbb{V}_k^{\text{div div}}(\begin{pmatrix} r_1^\vee \\ -1 \end{pmatrix}, \mathbf{r}_2; \mathbb{S}) = \mathbb{V}_{k-2}^{L^2}(\mathbf{r}_2).$$

On the other side,

$$\begin{aligned} & \dim \mathbb{V}_k^{\text{div div}}(\begin{pmatrix} r_1^\vee \\ -1 \end{pmatrix}, \mathbf{r}_2; \mathbb{S}) - \dim \mathbb{V}_{k-2}^{L^2}(\mathbf{r}_2) \\ &= 2 \binom{r_1^\vee + 3}{2} |\Delta_0(\mathcal{T}_h)| + 2(k - 2r_1^\vee - 2) |\Delta_1(\mathcal{T}_h)| \\ & \quad + |\Delta_2(\mathcal{T}_h)| \dim \mathbb{B}_k(\begin{pmatrix} r_1^\vee \\ -1 \end{pmatrix}) + |\Delta_2(\mathcal{T}_h)| \dim \mathbb{B}_{k+2}(\begin{pmatrix} r_1^\vee + 2 \\ 1 \end{pmatrix}) - |\Delta_2(\mathcal{T}_h)| \\ & \quad - 3(|\Delta_0(\mathcal{T}_h)| - |\Delta_1(\mathcal{T}_h)| + |\Delta_2(\mathcal{T}_h)|). \end{aligned}$$

Thanks to the DoFs (21)-(23) for $\mathbb{V}_{k+1}^{\text{curl}}(\begin{pmatrix} r_1^\vee + 1 \\ 0 \end{pmatrix}; \mathbb{R}^2)$ and the Euler's formula,

$$\dim \mathbb{V}_k^{\text{div div}}(\begin{pmatrix} r_1^\vee \\ -1 \end{pmatrix}, \mathbf{r}_2; \mathbb{S}) - \dim \mathbb{V}_{k-2}^{L^2}(\mathbf{r}_2) = \dim \mathbb{V}_{k+1}^{\text{curl}}(\begin{pmatrix} r_1^\vee + 1 \\ 0 \end{pmatrix}; \mathbb{R}^2) - 3,$$

which together with Lemma 2.1 ends the proof. \square

Example 5.18. When $r_1^\vee = 0$ and $\mathbf{r}_2 = -1$, we recover the finite element divdiv complex constructed in [14]

$$\mathbf{RT} \xrightarrow{\subset} \text{Herm}_{k+1}(\begin{pmatrix} 1 \\ 0 \end{pmatrix}; \mathbb{R}^2) \xrightarrow{\text{sym curl}} \text{CH}_k(\begin{pmatrix} 0 \\ -1 \end{pmatrix}) \xrightarrow{\text{div div}} \text{DG}_{k-2}(\begin{pmatrix} -1 \\ -1 \end{pmatrix}) \rightarrow 0.$$

Remark 5.19. The first finite element divdiv complex constructed in [12]

$$\mathbf{RT} \xrightarrow{\subset} \text{Lagrange}_{k+1}(\begin{pmatrix} 0 \\ 0 \end{pmatrix}; \mathbb{R}^2) \xrightarrow{\text{sym curl}} \text{HHJ}_k \xrightarrow{\text{div div}} \text{Lagrange}_{k+1}(\begin{pmatrix} 0 \\ 0 \end{pmatrix}) \rightarrow 0$$

is based on the divdiv complex

$$\mathbf{RT} \xrightarrow{\subset} \mathbf{H}^1(\Omega; \mathbb{R}^2) \xrightarrow{\text{sym curl}} \mathbf{H}^{-1}(\text{div div}, \Omega; \mathbb{S}) \xrightarrow{\text{div div}} H^{-1}(\Omega) \rightarrow 0$$

and is not covered in this paper.

REFERENCES

- [1] J. Argyris, I. Fried, and D. Scharpf. The TUBA family of plate elements for the matrix displacement method. *Aero. J. Roy. Aero. Soc.*, 72:701–709, 1968. 13
- [2] D. Arnold, R. Falk, and R. Winther. Finite element exterior calculus: from Hodge theory to numerical stability. *Bull. Amer. Math. Soc. (N.S.)*, 47(2):281–354, 2010. 1
- [3] D. N. Arnold. *Finite element exterior calculus*, volume 93 of *CBMS-NSF Regional Conference Series in Applied Mathematics*. Society for Industrial and Applied Mathematics (SIAM), Philadelphia, PA, 2018. 1, 3
- [4] D. N. Arnold, R. S. Falk, and R. Winther. Differential complexes and stability of finite element methods. II. The elasticity complex. In *Compatible spatial discretizations*, volume 142 of *IMA Vol. Math. Appl.*, pages 47–67. Springer, New York, 2006. 5, 22

- [5] D. N. Arnold, R. S. Falk, and R. Winther. Finite element exterior calculus, homological techniques, and applications. *Acta Numer.*, 15:1–155, 2006. [1](#), [14](#)
- [6] D. N. Arnold, R. S. Falk, and R. Winther. Geometric decompositions and local bases for spaces of finite element differential forms. *Computer Methods in Applied Mechanics and Engineering*, 198(21–26):1660–1672, 2009. [7](#), [9](#)
- [7] D. N. Arnold and K. Hu. Complexes from complexes. *Found. Comput. Math.*, 2021. [1](#), [2](#), [5](#), [22](#), [23](#), [27](#)
- [8] D. N. Arnold and R. Winther. Mixed finite elements for elasticity. *Numer. Math.*, 92(3):401–419, 2002. [5](#), [22](#)
- [9] I. N. Bernšteĭn, I. M. Gelfand, and S. I. Gelfand. Differential operators on the base affine space and a study of g -modules. In *Lie groups and their representations (Proc. Summer School, Bolyai János Math. Soc., Budapest, 1971)*, pages 21–64, 1975. [5](#)
- [10] J. H. Bramble and M. Zlámal. Triangular elements in the finite element method. *Math. Comp.*, 24:809–820, 1970. [6](#), [13](#)
- [11] F. Brezzi, J. Douglas, Jr., and L. D. Marini. Two families of mixed finite elements for second order elliptic problems. *Numer. Math.*, 47(2):217–235, 1985. [18](#)
- [12] L. Chen, J. Hu, and X. Huang. Multigrid methods for Hellan–Herrmann–Johnson mixed method of Kirchhoff plate bending problems. *Journal of Scientific Computing*, 76(2):673–696, 2018. [33](#)
- [13] L. Chen and X. Huang. Decoupling of mixed methods based on generalized Helmholtz decompositions. *SIAM J. Numer. Anal.*, 56(5):2796–2825, 2018. [1](#)
- [14] L. Chen and X. Huang. Finite elements for divdiv-conforming symmetric tensors. *arXiv preprint arXiv:2005.01271*, 2020. [3](#), [29](#), [33](#)
- [15] L. Chen and X. Huang. A finite element elasticity complex in three dimensions. *Math. Comp.*, 2021. [2](#), [3](#), [16](#), [23](#), [29](#)
- [16] L. Chen and X. Huang. Finite elements for div and divdiv conforming symmetric tensors in arbitrary dimension. *arXiv preprint arXiv:2106.13384*, 2021. [16](#)
- [17] L. Chen and X. Huang. Geometric decomposition of div-conforming finite element tensors. *arXiv preprint arXiv:2112.14351*, 2021. [17](#)
- [18] L. Chen and X. Huang. Geometric decompositions of the simplex lattice and smooth finite elements in arbitrary dimension. *arXiv preprint arXiv:2111.10712*, 2021. [6](#)
- [19] S. H. Christiansen, J. Hu, and K. Hu. Nodal finite element de Rham complexes. *Numer. Math.*, 139(2):411–446, 2018. [2](#), [17](#), [19](#), [22](#)
- [20] S. H. Christiansen and K. Hu. Finite element systems for vector bundles: Elasticity and curvature. *Found. Comput. Math.*, 2022. [3](#)
- [21] M. Costabel and A. McIntosh. On Bogovskĭĭ and regularized Poincaré integral operators for de Rham complexes on Lipschitz domains. *Math. Z.*, 265(2):297–320, 2010. [30](#)
- [22] M. Eastwood. A complex from linear elasticity. In *The Proceedings of the 19th Winter School “Geometry and Physics” (Srnt, 1999)*, pages 23–29, 2000. [5](#)
- [23] R. S. Falk and M. Neilan. Stokes complexes and the construction of stable finite elements with pointwise mass conservation. *SIAM J. Numer. Anal.*, 51(2):1308–1326, 2013. [2](#), [16](#), [21](#)
- [24] R. Fan, Y. Liu, and S. Zhang. Mixed schemes for fourth-order DIV equations. *Comput. Methods Appl. Math.*, 19(2):341–357, 2019. [21](#)
- [25] J. Hu, T. Lin, and Q. Wu. A construction of C^r conforming finite element spaces in any dimension. *arXiv:2103.14924*, 2021. [13](#)
- [26] J. Hu, R. Ma, and M. Zhang. A family of mixed finite elements for the biharmonic equations on triangular and tetrahedral grids. *Sci. China Math.*, 64(12):2793–2816, 2021. [3](#), [32](#)
- [27] K. Hu, Q. Zhang, and Z. Zhang. Simple curl-curl-conforming finite elements in two dimensions. *SIAM J. Sci. Comput.*, 42(6):A3859–A3877, 2020. [2](#), [21](#)
- [28] M.-J. Lai and L. L. Schumaker. *Spline functions on triangulations*, volume 110. Cambridge University Press, 2007. [13](#)
- [29] Y. Liao, P. Ming, and Y. Xu. Taylor-Hood like finite elements for nearly incompressible strain gradient elasticity problems. *arXiv preprint arXiv:2105.00144*, 2021. [16](#)
- [30] J. Morgan and R. Scott. A nodal basis for C^1 piecewise polynomials of degree $n \geq 5$. *Math. Comput.*, 29:736–740, 1975. [13](#)
- [31] R. Stenberg. A nonstandard mixed finite element family. *Numer. Math.*, 115(1):131–139, 2010. [17](#)
- [32] A. Ženišek. Interpolation polynomials on the triangle. *Numer. Math.*, 15:283–296, 1970. [13](#)

DEPARTMENT OF MATHEMATICS, UNIVERSITY OF CALIFORNIA AT IRVINE, IRVINE, CA 92697, USA
Email address: chenlong@math.uci.edu

SCHOOL OF MATHEMATICS, SHANGHAI UNIVERSITY OF FINANCE AND ECONOMICS, SHANGHAI 200433,
CHINA
Email address: huang.xuehai@sufe.edu.cn